Microstructural, mechanical, and tribological evaluation of thermally sprayed wear-resistant coatings for aerospace applications

Cyrus Bidmeshki

A Thesis

In the department of

Mechanical, Industrial, and Aerospace Engineering

Presented in Partial Fulfillment of the

Requirements for the Degree of

Master of Applied Science (Mechanical Engineering)

at

Concordia University

Montréal, Québec; Canada

May 2023

CONCORDIA UNIVERSITY

School of Graduate Studies

This is to certify that the thesis prepared

By: **Cyrus Bidmeshki**

Entitled: **Microstructural, mechanical, and tribological evaluation of thermally sprayed wear-resistant coatings for aerospace applications**

and submitted in partial fulfillment of the requirements for the degree of

Master of Applied Science (Mechanical Engineering)

complies with the regulation of the University and meets the accepted standard with respect to originality and quality.

Signed by the final examining committee:

_____ Chair
Dr. Martin Pugh

_____ Examiner
Dr. Rolf Wuthrich

_____ Examiner
Dr. Martin Pugh

_____ Supervisor
Dr. Pantcho Stoyanov

_____ Supervisor
Dr. Christian Moreau

Approved by _____

Martin. Pugh, Chair
Department of Mechanical, Industrial and Aerospace Engineering

May, 03 2023 _____

Mourad Debbabi, Dean
Gina Cody School of Engineering and Computer Science

Abstract

Microstructural, mechanical, and tribological evaluation of thermally sprayed wear-resistant coatings for aerospace applications

Cyrus Bidmeshki

Thermal sprayed tribological coatings have been used extensively in aerospace applications, primarily to overcome critical challenges such as abrasive wear, corrosion, erosion, oxidation and fatigue at high temperatures and pressures. Such coatings can also play a critical role in optimizing the efficiency of gas turbine engines, thereby reducing fuel consumption and CO2 emissions. High Velocity Oxy-Fuel (HVOF) thermal spraying with its higher gas jet velocity and lower flame temperature as compared to Air Plasma Spray (APS) is a promising deposition technique that can be used to deposit nickel- and copper- based tribological coatings. More specifically, dense coatings with lower oxide content and higher hardness have made this process a promising technique for producing wear resistant coatings capable of operating effectively in extreme environments.

The main objective of this research is to study the tribological properties of NiGraphite and Cu-Al systems deposited by HVOF and APS deposition processes in order to compare and determine the most suitable thermal spraying parameters. This work consists of two research studies, the first of which focuses on the tribological performance of HVOF-sprayed nickel graphite coatings with different compositions at room temperature and 450 °C. The second study evaluates the temperature response (room temperature, 300 °C and 450 °C) on the hardness and sliding wear behavior of Cu-10Al coatings deposited by HVOF and APS.

In both studies, the tribological tests were performed using a ball-on-flat tribometer and the wear profiles were extracted using a laser confocal microscope. Ex-situ characterization of the coatings was performed using scanning electron microscopy (SEM), energy dispersive spectroscopy (EDS), X-ray diffraction (XRD), image analysis, and Vickers microhardness testing at room and elevated temperatures. The HVOF 75Ni-25Gr coating showed the lower wear rates compared to 85Ni-15Gr at 450°C, while the wear rates of both coatings were similar at room

temperature. The APS Cu-10Al coating showed better wear resistance compared to the HVOF coating at all test temperature.

Acknowledgement

I would like to express my immense gratitude towards my supervisors, Dr. Christian Moreau, and Dr. Pantcho Stoyanov for providing me an opportunity to work on such an interesting research project. This project turned out to be a huge success due to their unconditional support, expert guidance, and enthusiastic mentorship. I would also like to appreciate the contributions of Dr. Richard R. Chromik, Dr. Fadhel Ben Ettouil, Dr. Sima Alidokht, and Dr. Andre C. Liberati for collaborating in this research work and supporting the study by providing valuable reviews.

I would like to thank all the members of the Thermal Spray Laboratory group for providing expert knowledge and guidance throughout my experiments. I also appreciate the technical assistance of Dr. Dmytro Kevorkov in experimental work. I specially thank Mr. Payank Patel, Mr. Amit Roy, Mrs Alejandra Islas Encalada and Miss Maya Harfouche for helping me throughout my research and for their excellent mentorship.

I am grateful to Concordia University for providing a platform and resources to carry out my valuable research in an effective way.

Finally, I would like to appreciate the support and motivation I received from my parents, siblings, and thermal spraying and tribology group members throughout my academic career.

Contribution of Authors

This thesis composes of peer-reviewed and under-review research articles. All the manuscripts have been produced by me as a principal author and my supervisors, Dr. Pantcho Stoyanov and Dr. Christian Moreau as co-authors in collaboration with others. Most of the experimental and technical writing work was performed by the principal author while the supervisor aided in providing analytical vision and technical guidance over the project. I acknowledge the contribution of the co-authors of the produced articles:

- Chapter 3: Bidmeshki, C.; Liberati, A.; Harfouche, M.; Ben Ettouil, F.; Alidokht, S.; Chromik, R.; Stoyanov, P; Moreau, C. Microstructural, mechanical, and tribological properties of HVOF sprayed Ni-Graphite coatings. Submitted to Journal of X.

• Bidmeshki C was responsible for conducting an in-depth literature review, conceptualization, methodology, experiments, analysis, writing the original manuscript draft, and revising the final manuscript. Ben Ettouil F was responsible for optimising the HVOF technique parameters. Chromik R, Alidokht S, and Harfouche M were responsible for Hardness test and SEM analysis. Liberati A was responsible for providing a critical review of the manuscript and addressing the shortcomings of the original draft. Moreau C and Stoyanov P were responsible for Conceptualization, guidance, interpretation of results and review of the manuscript.

- Chapter 4: Bidmeshki, C.; Liberati, A.; Roy, A.; Encalada Islas, A.; Ben Ettouil, F.; Alidokht, S.; Chromik, R.; Moreau, C; Stoyanov, P. Microstructural, mechanical, and tribological evaluation of CuAl-based coatings deposited by APS and HVOF.

• Bidmeshki C was responsible for conducting an in-depth literature review, conceptualization, methodology, experiments, analysis, writing the original manuscript draft, and revising the final manuscript. Ben Ettouil F was responsible for optimising the HVOF technique parameters. Chromik R, Alidokht S, and Encalada Islas A were responsible for Hardness test. Liberati A and Roy A was responsible for providing a critical review of the manuscript and addressing the shortcomings of the original draft. Stoyanov P and Moreau C were responsible for conceptualization, guidance, interpretation of results and review of the manuscript.

Table of Contents

List of Figures

List of Tables

Abbreviations

HVOF – High Velocity Oxygen Fuel

APS – Atmospheric Plasma Spraying

SEM – Scanning Electron Microscopy

EDS – Electron Dispersive Spectroscopy

XRD – X-ray Diffraction

COF – Coefficient of Friction

Organization of thesis

i. Chapter 1 presents the introduction along with the motivation and scope of the thesis.

ii. Chapter 2 provides background information on thermal spraying and tribology. Additionally, a literature review on tribological coatings with emphasis on metallic abradable coatings is presented.

iii. Chapter 3 presents the microstructural, mechanical, and tribological evaluation of HVOF sprayed nickel graphite coatings in room and higher temperatures.

iv. Chapter 4 presents the microstructural, mechanical, and tribological study of APS and HVOF sprayed CuAl-based coatings at room and higher temperatures.

v. Chapter 5 highlights the overall major conclusions and the future work on thermally sprayed tribological coatings.

Chapter

1. INTRODUCTION & SCOPE

In this chapter…

The motivation and brief introduction to the thesis is presented with its objectives.

1.1 Introduction

Engineering components used in the demanding environment of aerospace gas turbines are susceptible to degradation by various failure mechanisms such as wear, erosion, corrosion, oxidation and fatigue [1-5]. The loss of material from contacting surfaces during their relative motion is referred to as wear [6]. In order to achieve durable, economical, and easy-to-implement new materials with high wear resistance properties, surface technology is the solution to protect such industrial parts under various tribological conditions [7]. Tribological coatings are thin layers of material applied to a surface to reduce wear and friction in general. These coatings can be used to improve the performance and lifetime of a wide range of mechanical components such as blades, bearings, gears and engine parts [8].

There are many different methods for developing tribological coatings, and the choice of method depends on the specific requirements of the application. Some common methods include physical vapor deposition (PVD), chemical vapor deposition (CVD), electroplating, electrospinning, and thermal spraying [9]. Thermal spraying uses a high-energy flame or plasma jet to melt a powdered material, which is then sprayed onto the substrate as a fine mist of molten or partially molten particles [5]. There are many other methods for developing tribological coatings, and researchers and engineers are constantly exploring new approaches to improve the performance and versatility of these coatings.

Nickel (Ni) - Graphite (Gr) composite coatings are potential protective materials used in gas turbine engines that consist of a combination of nickel and graphite. These coatings are often used to improve the wear and/or corrosion resistance of a surface. Ni-Graphite coatings are typically used in applications where wear resistance is important, such as tribological interfaces in gas engine components. Ni-Graphite coatings can be deposited by a variety of methods, including APS and electroplating [10]. They are typically used in applications where both wear resistance and low friction are important. The graphite in these coatings helps reduce friction, while the nickel provides wear resistance. Overall, Ni-Graphite coatings are effective in improving the performance of a wide range of mechanical components and are widely used in a variety of industries [11-16].

Cu-Al coatings, also known as copper-aluminum coatings, are metallic wear-resistant coatings applied to the surface of a substrate material using a process such as electroplating, vapor deposition, sputtering, thermal spraying and mechanochemical techniques [17-22]. The

combination of copper and aluminum in the coating can provide a number of benefits, such as improved wear resistance, corrosion resistance, and electrical conductivity. Cu-Al coatings are widely used in a variety of applications, including aerospace, automotive, and electronics manufacturing. They can be applied to a wide range of substrate materials, including metals, ceramics, and plastics. The properties of Cu-Al coatings can be tailored by adjusting the ratio of copper to aluminum in the coating, as well as the thickness of the coating [23,24]. For example, higher copper content can improve the corrosion resistance of the coating, while higher aluminum content can improve wear resistance and electrical conductivity. The choice of method used to apply Cu-Al coatings depends on the specific requirements of the application, including the desired thickness and properties of the coating, as well as the substrate material and availability of equipment.

Several studies have shown that Ni-Graphite coatings can be deposited by some of the most widely used thermal spray techniques such as cold spray, flame spray, and APS [11,13,25]. For Cu-Al coatings, APS has been the main deposition technique, although researchers have used electric spark, cathodic arc, and laser cladding methods to deposit this material [26-28]. However, HVOF has an advantage over these processes in that it can produce a thick and dense coating that is more suitable for tribological applications due to its higher hardness and stability. HVOF is a high-temperature deposition technique in which molten and semi-molten particles are sprayed onto the substrate in the form of splats.

While a considerable amount of research has been done on Ni-Graphite and Cu-Al coatings, their sliding wear behavior has received less attention. Very few articles can be found on the tribological evaluation of HVOF spraying of these coatings. The main purpose of this work is to critically evaluate HVOF spraying of these coatings.

1.2 Thesis objectives

The primary objective of this thesis is to develop nickel-graphite and copper-aluminum wear resistant coatings by means of HVOF for aerospace applications and to identify the tribological performance of these coatings at higher temperatures. The following specific objectives (SO) have been identified for this thesis:

SO1: Identify the sliding wear behavior of HVOF deposited Ni-Graphite coatings with two different chemical compositions (75Ni-25Gr and 85Ni-15Gr) at room and elevated temperatures.

SO2: Compare the tribological performance and hardness of Cu-Al coatings deposited by HVOF and APS thermal spraying at room and elevated temperatures.

References:

1. Bhushana Rao VN, Kumar IN, Prasad KB. Failure analysis of gas turbine blades in a gas turbine engine used for marine applications. Int J Eng Sci Tech. 2014 Feb 7;6(1):43–8.

2. Yin F, Rao AG. A review of gas turbine engine with inter-stage turbine burner. Progress in Aerospace Sciences. 2020 Feb;121:100695.

3. National Academies of Sciences EM, Sciences DEP, Board ASE, Turbines CATG. Advanced Technologies for Gas Turbines [Internet]. National Academies Press; 2020. Available from: https://books.google.ca/books?id=VJveDwAAQBAJ

4. Rugg D. Materials for future gas turbine applications. Materials Science and Technology. 2014 Dec;30(15):1848–52.

5. Handbook of Environmental Degradation of Materials [Internet]. Elsevier; 2018 [cited 2022 Dec 20]. Available from: https://linkinghub.elsevier.com/retrieve/pii/C20160020818

6. Laguna-Camacho JR, Villagrán-Villegas LY, Martínez-García H, Juárez-Morales G, Cruz-Orduña MI, Vite-Torres M, et al. A study of the wear damage on gas turbine blades. Engineering Failure Analysis. 2016 Mar;61:88–99.

7. Barshilia HC. Surface Modification Technologies for Aerospace and Engineering Applications: Current Trends, Challenges and Future Prospects. Trans Indian Natl Acad Eng. 2021 Jun;6(2):173–88.

8. Holmberg K, Matthews A, Ronkainen H. Coatings tribology—contact mechanisms and surface design. Tribology International. 1998 Jan;31(1–3):107–20.

9. Tribology and Characterization of Surface Coatings.

10. Soltani R, Heydarzadeh-Sohi M, Ansari M, Afsari F, Valefi Z. Effect of APS process parameters on high-temperature wear behavior of nickel–graphite abradable seal coatings. Surface and Coatings Technology. 2017 Jul;321:403–8.

11. Huang C, Li W, Xie Y, Planche MP, Liao H, Montavon G. Effect of Substrate Type on Deposition Behavior and Wear Performance of Ni-Coated Graphite/Al Composite Coatings Deposited by Cold Spraying. Journal of Materials Science & Technology. 2017 Apr;33(4):338–46.

12. Song SP, Li C, Ji ZH. Orthogonal Analysis on Hardness of Nickel/Graphite Sealing Coating. AMM. 2012 Apr;164:55–8.

13. Xue W, Gao S, Duan D, Wang L, Liu Y, Li S. Study on the High-Speed Rubbing Wear Behavior Between Ti6Al4V Blade and Nickel–Graphite Abradable Seal Coating. Journal of Tribology. 2017 Mar 1;139(2):021604.

14. Tang JJ, Liu K, Yang QZ, Wang YH, Zhang P, Wang Y, et al. The influence of size and distribution of graphite on the friction and wear behavior of Ni–graphite coatings. Surface and Coatings Technology. 2014 Aug;252:48–55.

15. Batra U. Thermal spray coating of abradable Ni based composite. Surface Engineering. 2009 May;25(4):284–6.

16. Lesnevskii LN, Lezhnev LYu, Lyakhovetskii MA, Troshin AE, Ushakov AM. Wear resistance of composite plasma coatings with graphite. J Mach Manuf Reliab. 2017 Jan;46(1):25–32.

17. Zhang J, Wang B hao, Chen G hong, Wang R min, Miao C hui, Zheng Z xiang, et al. Formation and growth of Cu–Al IMCs and their effect on electrical property of electroplated Cu/Al laminar composites. Transactions of Nonferrous Metals Society of China. 2016 Dec;26(12):3283–91.

18. Moon HK, Yoon J, Kim H, Lee NE. Cu-Al alloy formation by thermal annealing of Cu/Al multilayer films deposited by cyclic metal organic chemical vapor deposition. Met Mater Int. 2013 May;19(3):611–6.

19. Zhang P, Zhang JY, Li J, Liu G, Wu K, Wang YQ, et al. Combined effect of texture and nanotwins on mechanical properties of the nanostructured Cu and Cu–Al films prepared by magnetron sputtering. J Mater Sci. 2015 Feb;50(4):1901–7.

20. Harutyunyan VS, Torossyan AR, Aivazyan AP. Deformations, subgrain structure, dislocation arrangement and transition layer formation in Cu/Al coating deposited by mechanochemical technique. Applied Surface Science. 2004 Jan;222(1–4):43–64.

21. Zhu L, Zhang W, Zhang T, Qiu J, Cao J, Wang F. Effect of the Cu Content on the Microstructure and Corrosion Behavior of PEO Coatings on Al– *x* Cu Alloys. J Electrochem Soc. 2018;165(9):C469–83.

22. Lao ML, He J, Schweinfest R, Ruhle M, Levi CG, Lavernia EJ. Synthesis and Characterization of nanocrystalline Cu-Al coatings. Mater. Sci. Eng. A. 2003 Apr;347(1-2):231-242.

23. Stoyanov P, Harrington KM, Frye A. Insights into the Tribological Characteristic of Cu-Based Coatings Under Extreme Contact Conditions. JOM. 2020 Jun;72(6):2191–7.

24. Ren W, Mall S, Sanders JH, Sharma SK. Degradation of Cu-Al Coating on Ti-6AI-4V Substrate under Fretting Fatigue Conditions. Tribology Transactions. 2003 Jan;46(3):353–60.

25. Fang-Li Y, Yu B, Xiu-Ying W, Hai-Jun W, Jiu-Hui W. Corrosion Resistance and Anti-wear Property of Nickel Based Abradable Sealing Coating Deposited by Plasma Spraying. Journal of Inorganic Materials. 2016;31(7):687.

26. Pokhmurs'kyi VI, Student MM, Dovhunyk VM, Sydorak II. [No title found]. Materials Science. 2002;38(3):455–7.

27. Ren W, Mall S, Sanders JH, Sharma SK. Evaluation of coatings on Ti–6Al–4V substrate under fretting fatigue. Surface and Coatings Technology. 2005 Mar;192(2–3):177–88.

28. Lifan S, Yuan G, Dejun K. Effect of MoS2 mass fraction on microstructure and tribological characteristics of laser cladded Cu–10Al coating. Surfaces and Interfaces. 2022 Feb;28:101599.

Chapter

2. BASIC CONCEPTS & BACKGROUND

In this chapter…

A brief introduction to tribology involving the concepts of friction, wear and lubrication have been discussed and basic concept of thermal spraying technology has been presented. At the end, the most widely used thermally sprayed tribological coatings have been explained

2.1 A Brief History of Tribology

The study of tribology, or the science of interacting surfaces in relative motion, has a long history dating back to ancient times [1]. People have always been concerned with the performance and efficiency of tools and machines and have sought ways to reduce friction and wear. Friction and wear have been a concern for engineers and inventors throughout history because they can significantly affect the performance and efficiency of machines [2]. The ancient Egyptians, Greeks, and Romans all contributed to the field by developing ways to reduce friction and wear in their machines and tools. The term "tribology" was coined in 1966 by Peter Jost, a British engineer and tribologist. The word is derived from the Greek root "tribos," meaning "friction. In the early 19th century, the Industrial Revolution led to an increased need for more efficient machinery, which led to the development of new technologies and techniques to reduce friction and wear. In the 20th century, the study of tribology became more formalized, and tribologists began to use advanced techniques such as microscopy and computer modeling to study the behavior of materials under different conditions. Today, tribology is an important field with applications in many industries, including automotive, aerospace, and manufacturing. The study of tribology continues to advance, and researchers are constantly looking for new ways to improve machine performance and reduce wear and friction of materials.

2.2 What is Tribology?

Tribology is the study of the motion of surfaces relative to each other. This phenomenon has an enormous impact on the daily lives of people all over the world. There are many examples, such as when two different things rub together and cause a fire, when someone walks or runs, when they sweat on their hands or feet, which increases friction and makes it easier to walk or run, etc. Tribology in general consists of three core topics: friction, wear, and lubrication [3,4]. Wear has only recently begun to receive the same level of scientific attention as friction, which has been studied for about 300 years, and lubrication for more than a century. Friction and wear are caused by the loss of material due to resistance to relative motion. These phenomena are minimized by the use of lubricants, which can be either liquid or solid. This is a field that requires the skills of physicists, chemists, mechanical engineers, chemical engineers, materials scientists, and metallurgists because it draws on the expertise of all. Each topic of tribology is discussed in a continuum.

2.2.1 Friction

Friction is a force described as the resistance encountered by one body as it moves over another. This broad term encompasses the important relative motion classes of sliding and rolling. Although it is helpful to distinguish between sliding and rolling friction, the two are not mutually exclusive, and even what appears to be "pure" rolling almost always involves some sliding. In both ideal rolling and sliding, the upper body must be moved over the stationary counterpart, as shown in Figure 2.1, using a tangential force F [5].

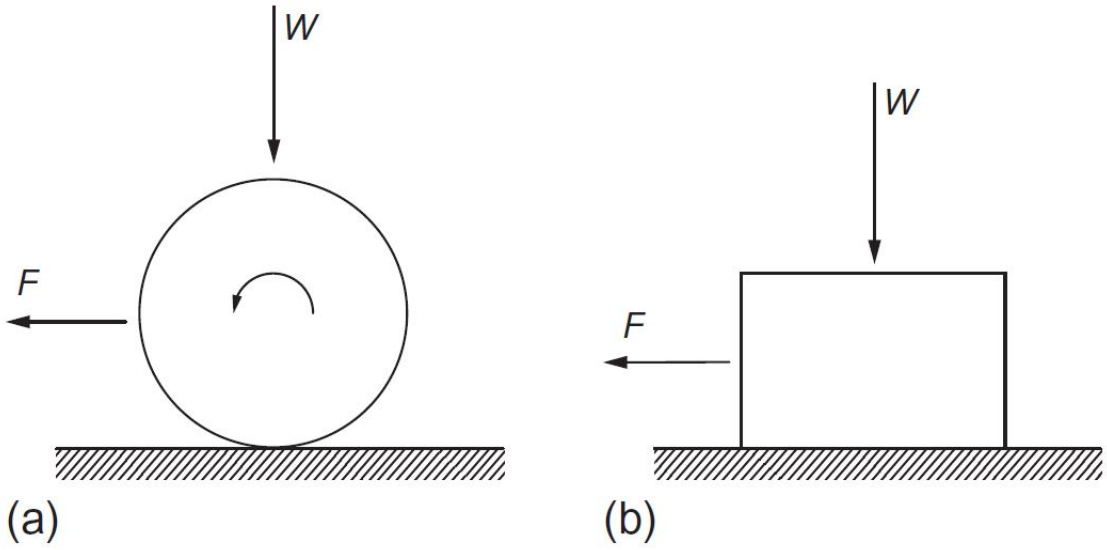

Figure 2. 1 A force, F, is needed to overcome friction and cause motion by (a) rolling or (b) sliding [5]

The coefficient of friction is the ratio of this frictional force to the normal load W, and it is generally symbolised by the symbol μ:

$$\mu = F/W \tag{2.1}$$

The value of the coefficient of friction, which ranges from about 0.001 for a lightly loaded rolling bearing to more than 10 for two equal clean metal surfaces moving in a vacuum, succinctly describes the magnitude of the frictional force. However, for most typical materials moving in air without lubricant, the value falls in the range of about 0.1 to 1 [5]. In extension, the frictional drive between the two objects can be categorized in two isolated ways: (1) based on the nearness or non-appearance of lubricating fluid between the contacting surfaces (dry and wet contact) and (2) based

on the current state of the framework, i.e., whether the objects are as of now in motion or at rest at that specific occasion (static and dynamic friction). Dry friction occurs when there is no lubricating fluid between the contact surfaces. Wet friction, on the other hand, occurs when there is a lubricating film between two contacting/moving surfaces. On the other hand, static friction exists between contact surfaces when the whole system is at rest, for example, when the surface is already in motion (sliding), when movement is initiated, when there is sliding friction. Sliding friction can be an advantage in some components such as brakes and clutches [2,3]. It can also be a disadvantage in pistons in engine blocks and gears.

2.2.2 Wear

Wear occurs when two solid surfaces (mating materials) slide against each other. The widely used term "sliding wear" can occur in either dry or lubricated conditions, but in several engineering applications and in many laboratory investigations, the surfaces interact in air without lubricant. The resulting wear is called dry sliding wear, even though it occurs in the presence of moisture and at ambient temperatures. There are many different types of wear that can affect materials, including abrasive, adhesive, fatigue, erosive (impact), tribochemical and oxidative. The type of wear a material experiences depends on the specific conditions it is exposed to, including the type of load and stress it is subjected to, the environment and temperature it is exposed to, and the material properties of the material itself. There are also other factors that can affect the wear of a material, including the hardness, strength and surface roughness of the material. To reduce material wear, it is often necessary to select a material with appropriate properties for the application, design the component to minimize the forces acting on it, and use protective coatings or lubricants to reduce the rate of wear [6,7].

2.2.3 Lubrication

Lubrication is the study and application of lubricants in engineering systems. In engineering, lubrication is used to reduce friction and wear in a wide range of applications, including mechanical systems, bearings, gears, and engines. Lubricants are used to reduce the amount of force required to move one surface over another, which can help extend the life of mechanical components and reduce energy consumption [8]. They are usually liquids or gases, but in some cases can be solids or semi-solids. In general, they work by creating a thin film between the two surfaces, reducing the amount of direct contact between them, which helps to reduce

friction and wear. There are many different types of lubricants that can be used for different applications, including oils, greases and dry film lubricants. The choice of lubricant depends on the specific requirements of the application, such as the type of load, the temperature and environment, and the material properties of the contacting surfaces [8,9].

2.3 What is Thermal Spray Technology?

Different manufacturing techniques can result in materials with different microstructures due to processing temperature, cooling rate and the presence of impurities. These in turn can result in different mechanical properties such as strength, ductility and toughness, which determine their friction and wear behavior. For example, materials produced by casting techniques, such as casting aluminum into engine blocks, typically have a more porous microstructure with lower strength and ductility compared to materials produced by forging techniques, such as forging steel into gears. Several modern alloy systems, such as nickel-, cobalt-, titanium- and aluminum-based alloys produced in bulk, have demonstrated promising wear properties under extreme conditions. However, when entire components are made from these alloys, it is likely that expensive alloy materials will be eliminated, and new alloying technologies will be required to develop new materials. For example, a Ni-based alloy is known for its superior strength and excellent wear resistance [10]. On the other hand, if aerospace components are manufactured using these alloys, the overall weight and economics of the parts will increase dramatically. A cost-effective solution to these problems is to use wear-resistant coatings to protect lighter, lower-cost metals instead of expensive bulk alloys that typically require aggressive cleaning. Wear-resistant coatings not only reduce the cost and weight of manufactured components, but also allow damaged parts to be repaired, often without disassembly, rather than replaced.

Thermal spraying is a coating process in which a heat source is used to melt or partially melt a powdered material, which is then sprayed onto a surface to form a coating [11]. Figure 2.2 shows the classification of thermal spray processes according to different types of energy sources [12]. The sprayed material can be in the form of powder, wire or rod, and the heat source can be a flame, arc or plasma jet. The coating material is typically fed into a spray gun that uses high-temperature (200-10,000K) gas or plasma to melt the material in the form of droplets and propel them at high speeds (50-1000 m/s) toward the surface to form a thick coating (>100 μm) [13]. The result is a coating that is uniformly applied and strongly bonded to the surface. The material can

be metallic or non-metallic, and the process can be used to coat a variety of surfaces, including metal, plastic and ceramic. Thermal spray coatings are used in a wide range of industries, including aerospace, automotive, construction and manufacturing. They are often used to increase the wear resistance, corrosion resistance, erosion resistance, thermal stability, or electrical conductivity of a surface. It is also used to repair and rebuild damaged parts and to build up worn surfaces [14]. There are several different types of thermal spray processes, including flame spray, plasma spray, detonation gun, and high velocity oxy-fuel (HVOF) spray. Each of these processes uses a different heat source and spraying technique, and each is suitable for different types of coatings and surfaces [15].

This thesis compares the tribological behavior of HVOF sprayed and APS sprayed coatings. Thus, these technologies have been discussed briefly in the following sub-sections.

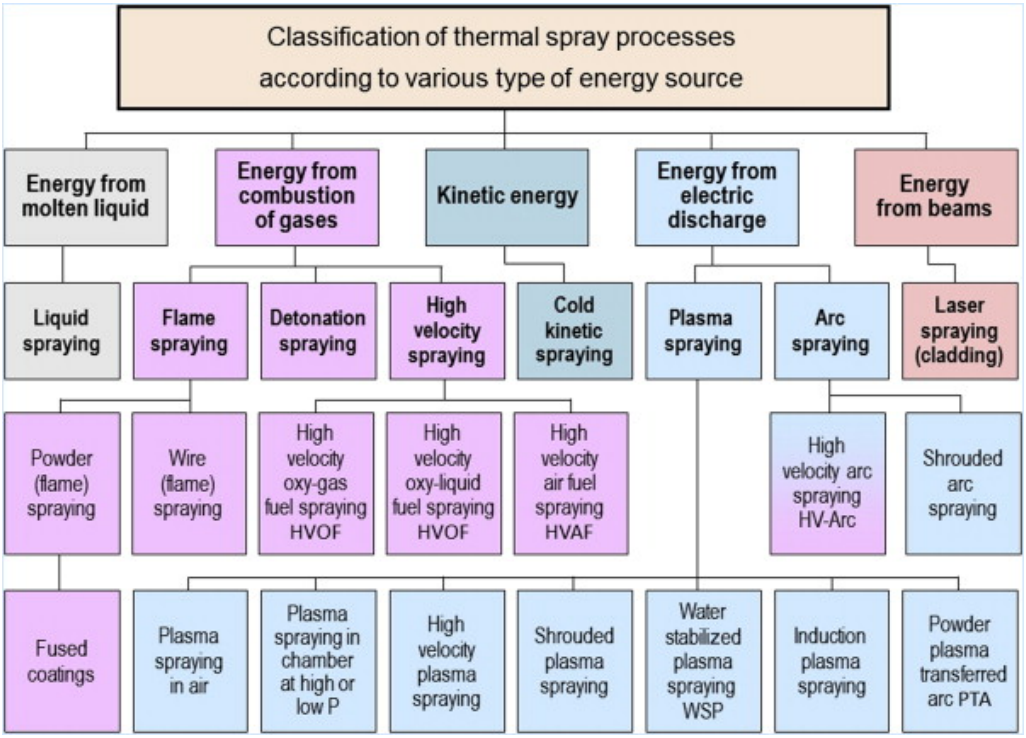

Figure 2. 2 Classification of thermal spray coating processes according to the type of energy source used in the process [12]

2.3.1 High Velocity Oxy-Fuel (HVOF)

High Velocity Oxygen Fuel (HVOF) is a combustion process used to spray metallic and ceramic coatings onto a variety of surfaces. It involves the use of a fuel, typically a hydrocarbon,

mixed with oxygen and injected into a combustion chamber to produce a high velocity stream (between 500 m/s and 2000 m/s) of hot gases. The resulting high-temperature ignited mixture flame (between 2200°C and 3000°C) is used to spray the coating material onto the surface. The coating material is typically in the form of a fine powder that is injected into the flame and melted by the heat. The molten material droplets are accelerated by the high velocity of the flame and sprayed onto the surface, although some of the unmelted or partially melted particles can be deposited due to high impact forces [11,16]. The resulting coating is of low porosity, similar to cold sprayed coatings, hard, wear resistant, and corrosion resistant. Used in the aerospace, automotive, and energy industries to improve the performance and life of machinery and equipment, HVOF coatings are often applied to parts subject to high wear, such as engine parts, bearings, and valve seats. It is also used to repair damaged surfaces and build up worn areas [17]. The resulting coatings are often of high quality and have excellent performance characteristics. In addition, the coatings produced by HVOF are typically very smooth and have high bond strength and adhesion to the substrate. Figure 2.3 shows a schematic diagram of HVOF technology [18]. In some applications, oxyacetylene fuel is used or simply air is used for combustion. It is well known that High Velocity Air Fuel (HVAF) spraying is one of the many variations of High Velocity Oxygen Fuel (HVOF) spraying, which uses air as the primary fuel for combustion.

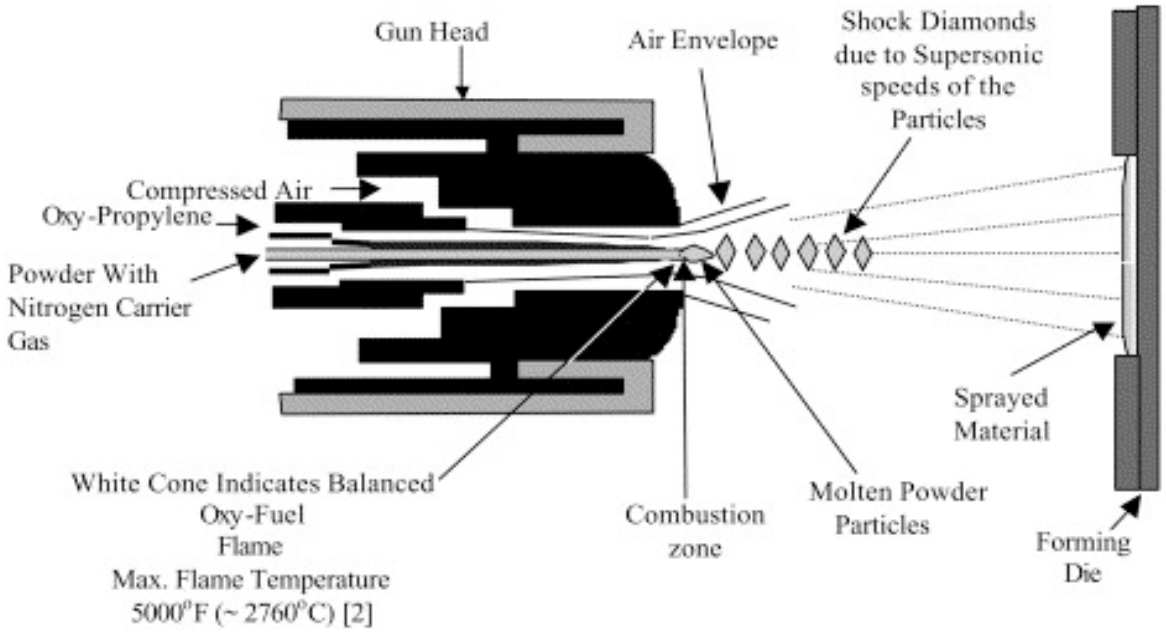

Figure 2. 3 Schematic of HVOF spray technology [18].

2.3.2 Atmospheric Plasma Spraying

The plasma jet is generated by heating a gas to a high temperature (10,000K) using an electric arc and injecting it into a nozzle. The high-energy plasma jet is capable of melting a wide range of materials, including metals, ceramics, and polymers, and can be used to deposit coatings on various types of substrates, including those with complex geometries [19]. Atmospheric plasma spraying is a thermal spraying process used to deposit a layer of material on a substrate. Figure 2.4 shows a schematic of the APS deposition process [20]. It involves the use of a plasma jet to melt and accelerate a stream of particles toward the substrate, where they are deposited and solidify to form a coating. In APS, a plasma jet is created by using an electric current to ionize a gas, such as argon, nitrogen, hydrogen, helium, or mixtures of these, and heating it to a high temperature. The combination of gases used in conjunction with the current applied to the electrode determines the amount of heat produced. The powdered feedstock material is fed into the jet through a powder injector. The feedstock particles are melted by the high temperature of the plasma jet and accelerated to high velocities, forming a spray of molten particles that are directed toward the substrate. As the particles flatten, cool and solidify upon impact, they form lamellae. The accumulation of such lamellae (often called splats) results in the deposition of a uniform coating on the substrate [11]. One of the major advantages of APS is its ability to deposit coatings with high bond strength, high density, and good adhesion to the substrate. It is also capable of producing coatings with a wide range of microstructures, including amorphous, nanocrystalline, and microcrystalline structures, depending on the sprayed material and processing conditions [21]. Due to the higher temperature and lower velocity of the sprayed particles in APS, metallic particles typically experience more oxidation during spraying than in the HVOF process.

APS is widely used in a variety of industries where high quality, durable coatings are required. These include aerospace (gas turbine and airframe components), automotive and transportation, power generation (gas turbine components and casings), petrochemical, marine, medical and energy, as well as the repair and refurbishment of worn or damaged parts for applications. Resistance to abrasive, adhesive, fretting or sliding wear; corrosion resistance in acidic, alkaline and saline environments; resistance to chemical attack; thermally resistant or

conductive surfaces; oxidation resistance; erosion resistance; and low friction and lubricious surfaces are among the most common surface functionalities achieved with APS.

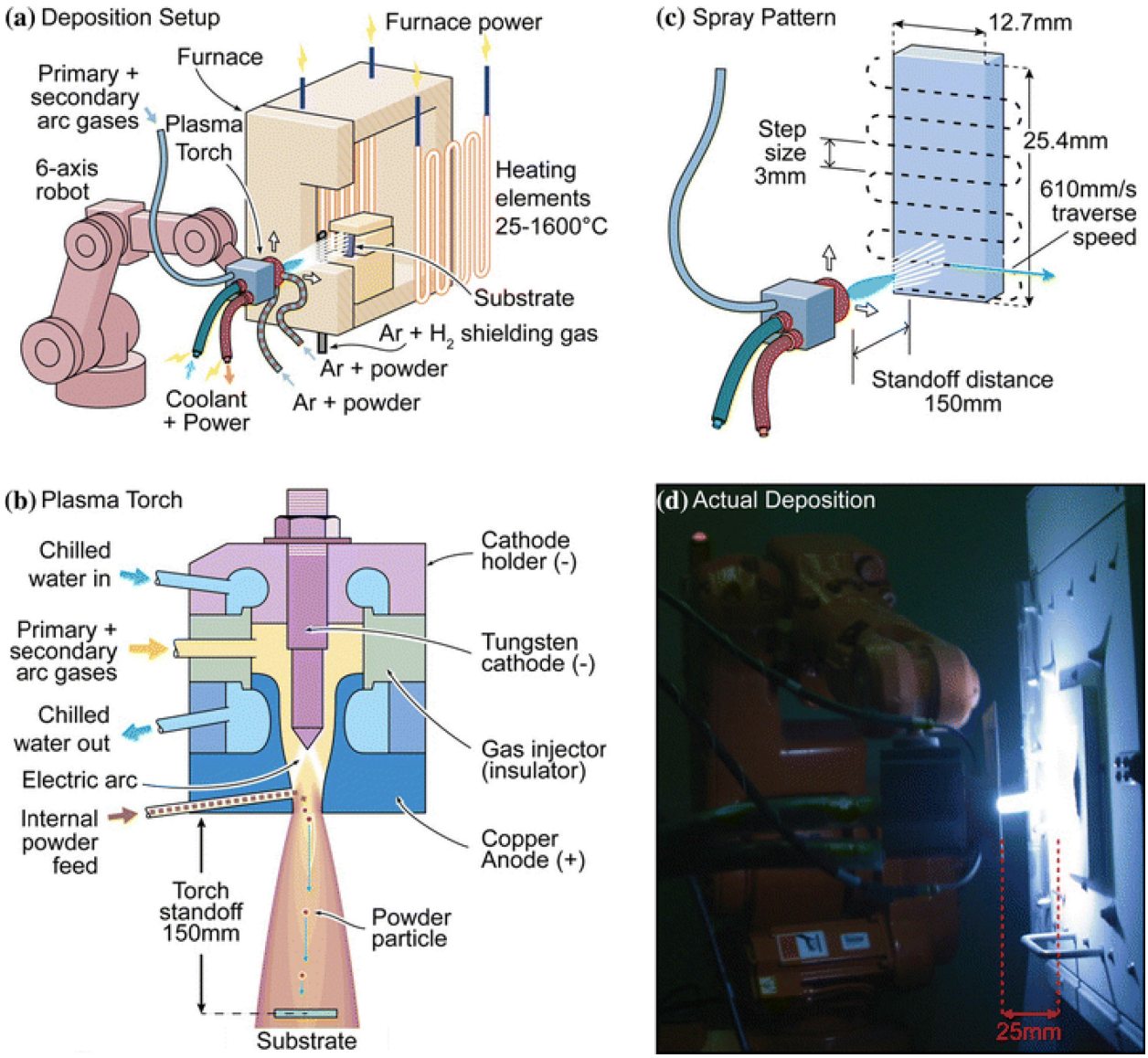

Figure 2. 4 a) Schematic illustration of the air plasma spray (APS) deposition. b) Schematic illustration of the plasma torch design. c) The spray pattern and definition of relevant deposition parameters. d) Photograph taken during APS deposition [20]

2.3.3 Thermally Sprayed Tribological Coatings

For optimum protection of metallic substrates, thermally sprayed abrasive or abradable tribological coatings can be applied, depending on the component application and operating

environment [22]. There is a recent trend in the production of tribological coatings that contain various types of additives to provide dry lubrication. Solid lubrication can be used to integrate or replace traditional liquid lubrication in cases where there are severe operating conditions such as high temperatures and high contact loads [23]. Metal-based coatings are commonly used for tribological applications. The available thermal deposition techniques with sufficient thermal or kinetic energy for this class of metallic materials range from plasma spray techniques to HVOF and detonation gun combustion systems to flame spraying. Abrasive metallic coatings, such as those based on aluminum, nickel, copper and cobalt, have been widely used for their wear resistance as well as for their protective role in the presence of thermal loads at higher temperatures.

2.3.3.1 Aluminum-based Tribological Coatings

Aluminum-based composite powders are often thermally sprayed in the low-pressure turbine stage of an aircraft engine, with operating temperatures up to 480 °C, with the goal of controlling clearance by producing exceptional friction properties [24,25].

2.3.3.1.1 Al-Si Polyester

Heterogeneous and porous aluminum-silicon-polyester coatings with low modulus, low hardness and high abradability are sprayed to minimize blade tip wear while providing excellent oxidation and good thermal shock resistance at temperatures up to 345°C. Aluminum as the metallic phase provides good bond strength and thermal properties, while polyester as a dislocator lowers the coefficient of friction and imparts friability to the coating [26-30].

2.3.3.1.2 Al-Si Graphite

Graphite-containing coatings, such as aluminum-silicon graphite, provide two important wear and erosion resistance properties at the same time. More specifically, graphite as a superior lubricant, with its layered structure and lack of polarity, also reduces the transfer of material from the coating to the rotating component. It should also be noted that they are equally suitable for maintenance and repair operations.

2.3.3.1.3 Al-(Si) hBN

Solid, self-lubricating Hexagonal Boron Nitride in Al-based coatings acts as a crack initiator, which in turn promotes chipping and reduces coating transfer to the blade tip. Highly inert Hexagonal Boron Nitride allows for higher temperature applications and helps the coating to wear easily at high speeds by reducing frictional heating on contact with the blades in medium and high-pressure compressors. It also helps weaken the interparticle bond strength within the Al-Si matrix for better friability [31-34].

2.3.3.4 Nickel-based Tribological Coatings

Nickel-based seal coatings are widely used in aerospace and gas path sealing systems in jet and industrial gas turbine (IGT) engines. The nickel-based powder can be used to produce coatings with properties that meet many design criteria by modifying the coating application parameters. For example, they can maintain their durability at high pressure and intermediate service temperatures up to 650°C. These coatings are suitable for rubbing against steel and nickel alloy blades, knives, or labyrinth seal strips such as those used in steam turbine balance piston applications (Sporer et al 2010). They are considered too abrasive for titanium blade applications (35,36).

2.3.3.2.1 Ni-Graphite

To improve compressor efficiency in aerospace jet engines, nickel graphite seal coatings have been widely used in friction-reducing bearing applications over the past several decades. These coatings, commonly used in the aerospace industry, are well suited for temperatures approaching 480°C and maintain their strength at intermediate temperatures (37-42).

2.3.3.2.2 Ni-Al (hexagonal) Boron Nitride

In nickel-aluminum hexagonal boron nitride, the Ni-Al metal matrix gives the coating strength, while the hBN decreases the friction. Depending on the application process, porosity in the coating may help to break the coating and keep the blade intact during rubbing [43].

2.3.3.2.3 Ni-Cr-Al Bentonite

Nickel-Chromium-Aluminum are hydrometallurgically clad composite powders consisting of a core of bentonite clay with a thin layer of alloyed NiCrAl. Compared to nickel graphite and nickel aluminum coatings, these coatings are not well suited for rubbing against titanium blades because they are too abrasive, but their application could be found in stationary parts of both gas and steam turbines against various components such as steel and nickel alloy blades, knives, or labyrinth seal strips. Although NiCrAl acts as the high-temperature resistant phase, bentonite is a calcined aluminum silicate mineral that provides the friability. The coating material also provides thermal barrier insulation properties and is also used to protect honeycomb brazed areas in engines [44].

2.3.3.2.4 Ni-Cr-Fe-Al (hexagonal) Boron Nitride

The last commercial type of Ni-based tribological coatings used in turbomachinery is nickel chromium iron aluminum hexagonal boron nitride. These mechanically clad composite powders consist of Ni-Cr alloy with Fe, Al and boron nitride refractory compounds. During thermal spraying, aluminum aids in the melting process as it undergoes an exothermic reaction with nickel (45). Like other solid lubricants, boron nitride helps the cutting process of the coating during blade penetration in accordance with the escalating oxidation resistance of it. It should also be added that the hexagonal form of Boron Nitride gives the solid lubricant properties similar to those of graphite.

2.3.3.3 Copper-based Tribological Coatings

Copper-based tribological coatings typically consist of a thin layer of copper or copper alloy and can be supplemented with other materials to improve their performance. They are known for their high wear resistance, low friction, good corrosion resistance and electrical conductivity, making them well suited for use in harsh environments on mechanical parts that are subject to high levels of sliding or rolling contact, such as bearings, gears and engine components. Copper-based tribological coatings are commonly used to reduce friction and wear. These coatings can also be used to improve the corrosion resistance and durability of the coated material [46].

2.3.3.3.1 Cu-Al-Fe (Polyester)

These coating materials have excellent resistance to abrasion and cavitation, as well as fretting and galling at low to moderate temperatures. They can be easily machined and finished to an excellent standard. They have excellent resistance to abrasion, cavitation, fretting and galling at low to moderate temperatures. These coatings should be used for soft bearing applications. Copper-aluminum-iron coatings can be used to produce surfaces that are resistant to moderate oxidation, wear and cavitation at low temperatures. It also has better corrosion resistance than pure copper materials [47-52].

2.3.3.3.3 Cu-Ni-(In)

Copper-Nickel coatings are designed to protect against metal-to-metal wear of engineered components, particularly titanium alloy components. Thermally deposited tribological coatings of this material are dense, low oxide and capable of reducing wear by fretting, adhesion, galling and cavitation. Cu-Ni containing indium improves the anti-galling and lubricity properties of the coating. Cu-Ni-In materials have been extensively used in the aerospace industry for anti-fretting wear applications approved by many major turbine engine manufacturers. APS and combustion powders are widely used to apply this coating and are used as sprayed for most applications due to the complexity of the part geometries [53,54].

2.3.3.4 Cobalt-based Tribological Coatings

2.3.3.4.1 Co-Ni-Cr-Al-Y (hexagonal) Boron Nitride - (Polyester)

Cobalt Nickel Chromium Aluminum Yttrium thermal sprayed powders with good oxidation and corrosion properties and high temperature friction behavior up to 750°C are usually combined with hexagonal boron nitride, bentonite, clay minerals and CaF2 as solid lubricants. As these types of abrasive coatings are stronger and harder than blades, their friability should be controlled by the presence of macroporosity up to 60% by volume fraction and this in turn could be run through various parameters of deposition methods [55].

References:

1. IV. On the theory of lubrication and its application to Mr. Beauchamp tower's experiments, including an experimental determination of the viscosity of olive oil. Phil Trans R Soc. 1886 Dec 31;177:157–234.

2. Stachowiak GW, Batchelor AW. Engineering tribology. Fourth edition. Amsterdam Heidelberg: Elsevier Butterworth-Heinemann; 2014. 852 p.

3. Bhushan B. Introduction to Tribology [Internet]. 1st ed. Wiley; 2013 [cited 2023 Jan 9]. Available from: https://onlinelibrary.wiley.com/doi/book/10.1002/9781118403259

4. Jamison WE. Introduction to tribology. Journal of Vacuum Science and Technology. 1976 Jan;13(1):76–81.

5. TRIBOLOGY: Friction and wear of engineering materials. Second Editions. Cambridge, MA: Elsevier; 2017. 388 p.

6. Holmberg K, Matthews A. Coatings tribology: properties, mechanisms, techniques and applications in surface engineering. 2nd ed. Amsterdam ; Boston: Elsevier Science; 2009. 560 p. (Tribology and interface engineering series).

7. Razavizadeh K, Eyre TS. Oxidative wear of aluminium alloys. Wear. 1982 Jul;79(3):325–33.

8. Ludema KC, Ajayi L. Friction, wear, lubrication: a textbook in tribology. Second edition. Boca Raton: Taylor & Francis, CRC Press; 2019.

9. Solid lubrication fundamentals and applications. Place of publication not identified: CRC Press; 2019.

10. Cabral Miramontes J, Pedraza Basulto GK, Gaona Tiburcio C, Zambrano Robledo PDC, Poblano Salas CA, Almeraya Calderón F. Coatings characterization of Ni-based alloy applied by HVOF. AEAT. 2018 Mar 5;90(2):336–43.

11. Tucker RC, editor. ASM handbook. 5A: Thermal spray technology / vol. ed. Robert C. Tucker. Materials Park, Ohio: ASM International; 2013. 398 p.

12. Vuoristo P. Thermal Spray Coating Processes. In: Comprehensive Materials Processing [Internet]. Elsevier; 2014 [cited 2023 Jan 7]. p. 229–76. Available from: https://linkinghub.elsevier.com/retrieve/pii/B9780080965321004076

13. Chandra S, Fauchais P. Formation of Solid Splats During Thermal Spray Deposition. J Therm Spray Tech. 2009 Jun;18(2):148–80.

14. Tribology and Characterization of Surface Coatings.

15. Barshilia HC. Surface Modification Technologies for Aerospace and Engineering Applications: Current Trends, Challenges and Future Prospects. Trans Indian Natl Acad Eng. 2021 Jun;6(2):173–88.

16. Tan JC, Looney L, Hashmi MSJ. Component repair using HVOF thermal spraying. Journal of Materials Processing Technology. 1999 Aug;92–93:203–8.

17. Dorfman MR. Thermal Spray Coatings. In: Handbook of Environmental Degradation of Materials [Internet]. Elsevier; 2018 [cited 2022 Dec 21]. p. 469–88. Available from: https://linkinghub.elsevier.com/retrieve/pii/B978032352472800023X

18. Stokes J, Looney L. HVOF system definition to maximise the thickness of formed components. Surface and Coatings Technology. 2001 Nov;148(1):18–24.

19. Nikiforov A, Chen Z, editors. Atmospheric Pressure Plasma - from Diagnostics to Applications [Internet]. IntechOpen; 2019 [cited 2023 Jan 9]. Available from: https://www.intechopen.com/books/atmospheric-pressure-plasma-from-diagnostics-to-applications

20. Richards BT, Zhao H, Wadley HNG. Structure, composition, and defect control during plasma spray deposition of ytterbium silicate coatings. J Mater Sci. 2015 Dec;50(24):7939–57.

21. Singh H, Sidhu BS, Puri D, Prakash S. Use of plasma spray technology for deposition of high temperature oxidation/corrosion resistant coatings – a review. Materials and Corrosion. 2007 Feb;58(2):92–102.

22. Bakshi SR, Harimkar SP. Surface Engineering for Extreme Conditions. JOM. 2015 Jul;67(7):1526–7.

23. Donnet C, Erdemir A. Solid Lubricant Coatings: Recent Developments and Future Trends. Tribology Letters. 2004 Oct;17(3):389–97.

24. Cappella A, Vincent J, Philippon S, Faure L. High-Speed Contact Study between a Ti-6-Al-4V Tool and an Abradable Coating Using Ballistic Benches and a Dynamic Compensation Approach. J Frict Wear. 2017 Nov;38(6):444–9.

25. Liu J, Yu Y, Liu T, Cheng X, Shen J, Li C. The Influence of Composition and Microstructure on the Abradability of Aluminum-Based Abradable Coatings. J Therm Spray Tech. 2017 Aug;26(6):1095–103.

26. Zhang N, Shen J, Xuan H, Hu Y, Hong W. Evaluation of an AlSi-polyester abradable seal coating performance using high-temperature and high-velocity abrasion tests. Proceedings of the Institution of Mechanical Engineers, Part J: Journal of Engineering Tribology. 2016 Jul;230(7):842–51.

27. Skiba S, Faure L, Philippon S, Papasidero J. Experimental Investigation of the Mechanical Behavior of an AlSi-PE Abradable Coating at High Strain Rates for a Large Range of Temperatures. J dynamic behavior mater. 2020 Jun;6(2):213–23.

28. Tang J jiang, Yu F li, Zhang H hong, Chen D. Effect of Microstructure Refining on the Thermal Stability and Wear Resistance of Abradable AlSi-Polyester Coating. J Therm Spray Tech. 2021 Aug;30(6):1615–23.

29. Jech D, Čelko L, Komarov P, Ziegelheim J, Česánek Z, Schubert J. The Role of Different Atmospheric Plasma Spray Parameters on Microstructure of Abradable AlSi-Polyester Coatings. SSP. 2017 Nov;270:224–9.

30. Martinet B, Cappella A, Philippon S, Montebello C. Effect of temperature on wear mechanisms of an aluminium - based abradable coating for aircraft engines after a dynamic interaction with a Ti6Al4V blade. Wear. 2020 Apr;446–447:203202.

31. Fois N, Watson M, Stringer J, Marshall M. An investigation of the relationship between wear and contact force for abradable materials. Proceedings of the Institution of Mechanical Engineers, Part J: Journal of Engineering Tribology. 2015 Feb;229(2):136–50.

32. Xue W, Gao S, Duan D, Zhang J, Liu Y, Li S. Effects of blade material characteristics on the high-speed rubbing behavior between Al-hBN abradable seal coatings and blades. Wear. 2018 Sep;410–411:25–33.

33. Xue W, Gao S, Duan D, Zhang J, Liu Y, Li S. Material Transfer Behavior between a Blade and Two Types of Coating during High-Speed Rubbing. Tribology Transactions. 2018 Sep 3;61(5):827–41.

34. Liu T, Yu YG, Shen J, Liu JM, Lu QY. Study on Wear Mechanism of an AlSi–Hexagonal Boron Nitride Abradable Seal Coating. AMR. 2015 Mar;1095:655–61.

35. Batra U. Thermal spray coating of abradable Ni based composite. Surface Engineering. 2009 May;25(4):284–6.

36. Fang-Li Y, Yu B, Xiu-Ying W, Hai-Jun W, Jiu-Hui W. Corrosion Resistance and Anti-wear Property of Nickel Based Abradable Sealing Coating Deposited by Plasma Spraying. Journal of Inorganic Materials. 2016;31(7):687.

37. Soltani R, Heydarzadeh-Sohi M, Ansari M, Afsari F, Valefi Z. Effect of APS process parameters on high-temperature wear behavior of nickel–graphite abradable seal coatings. Surface and Coatings Technology. 2017 Jul;321:403–8.

38. Huang C, Li W, Xie Y, Planche MP, Liao H, Montavon G. Effect of Substrate Type on Deposition Behavior and Wear Performance of Ni-Coated Graphite/Al Composite Coatings Deposited by Cold Spraying. Journal of Materials Science & Technology. 2017 Apr;33(4):338–46.

39. Song SP, Li C, Ji ZH. Orthogonal Analysis on Hardness of Nickel/Graphite Sealing Coating. AMM. 2012 Apr;164:55–8.

40. Xue W, Gao S, Duan D, Wang L, Liu Y, Li S. Study on the High-Speed Rubbing Wear Behavior Between Ti6Al4V Blade and Nickel–Graphite Abradable Seal Coating. Journal of Tribology. 2017 Mar 1;139(2):021604.

41. Tang JJ, Liu K, Yang QZ, Wang YH, Zhang P, Wang Y, et al. The influence of size and distribution of graphite on the friction and wear behavior of Ni–graphite coatings. Surface and Coatings Technology. 2014 Aug;252:48–55.

42. Lesnevskii LN, Lezhnev LYu, Lyakhovetskii MA, Troshin AE, Ushakov AM. Wear resistance of composite plasma coatings with graphite. J Mach Manuf Reliab. 2017 Jan;46(1):25–32.

43. Xue W, Gao S, Duan D, Zhang J, Liu Y, Li S. Ti6Al4V Blade Wear Behavior During High-Speed Rubbing with NiAl-hBN Abradable Seal Coating. J Therm Spray Tech. 2017 Feb;26(3):539–53.

44. Taylor TA, Thompson BW, Aton W. High speed rub wear mechanism in IN-718 vs. NiCrAl–Bentonite. Surface and Coatings Technology. 2007 Dec;202(4–7):698–703.

45. Raghavan V. Al-Cr-Fe-Ni (Aluminum-Chromium-Iron-Nickel). J Phase Equilib Diffus. 2011 Jun;32(3):253–4.

46. Gassot H, Junquera T, Ji V, Jeandin M, Guipont V, Coddet C, et al. Comparative Study of Mechanical Properties and Residual Stress Distributions of Copper Coatings Obtained by Different Thermal Spray Processes. Surface Engineering. 2001 Aug;17(4):317–22.

47. Ren W, Mall S, Sanders JH, Sharma SK. Degradation of Cu-Al Coating on Ti-6AI-4V Substrate under Fretting Fatigue Conditions. Tribology Transactions. 2003 Jan;46(3):353–60.

48. Jin O, Mall S, Sanders JH, Sharma SK. Durability of Cu–Al coating on Ti–6Al–4V substrate under fretting fatigue. Surface and Coatings Technology. 2006 Oct;201(3–4):1704–10.

49. Ren W, Mall S, Sanders JH, Sharma SK. Evaluation of coatings on Ti–6Al–4V substrate under fretting fatigue. Surface and Coatings Technology. 2005 Mar;192(2–3):177–88.

50. Jin O, Mall* S, Sanders JH, Sharma SK, Hager CH. Fretting Fatigue Behavior of Cu-Al-Coated Ti-6Al-4V. Tribology Transactions. 2007 Oct 23;50(4):497–506.

51. Lee H, Mall S, Murray KN. Fretting Wear Behavior of Cu–Al Coating on Ti-6Al-4V Substrate under Dry and Wet (Lubricated) Contact Condition. Tribol Lett. 2007 Aug 21;28(1):19–25.

52. Stoyanov P, Harrington KM, Frye A. Insights into the Tribological Characteristic of Cu-Based Coatings Under Extreme Contact Conditions. JOM. 2020 Jun;72(6):2191–7.

53. Hutson A. Effect of various surface conditions on fretting fatigue behavior of Ti–6Al–4V. International Journal of Fatigue. 2002 Dec;24(12):1223–34.

54. Fridrici V, Fouvry S, Kapsa P. Fretting wear behavior of a Cu–Ni–In plasma coating. Surface and Coatings Technology. 2003 Jan;163–164:429–34.

55. Botto D, Lavella M. High temperature tribological study of cobalt-based coatings reinforced with different percentages of alumina. Wear. 2014 Oct;318(1–2):89–97.

Chapter

3. MICROSTRUCTURAL, MECHANICAL, AND TRIBOLOGICAL EVALUATION OF NICKEL-GRAPHITE COATINGS DEPOSITED BY HVOF

In this chapter…

The tribological studies between two different compositions of Nickel-Graphite powders sprayed with high velocity oxy-fuel technique have been provided. The testing, characterization and data analysis was performed to understand the friction and wear behavior at varying temperatures

3.1 Abstract

High Velocity Oxy-Fuel (HVOF) is a widely used thermal spray deposition technique with higher gas jet velocity and lower flame temperature compared to traditional air plasma spray. In particular, this deposition process is promising for producing wear resistant coatings which are required to operate effectively in harsh conditions (e.g. gas turbine engines) such as high ranges of temperatures, high contact pressures, and erosive interaction of abrasive particles. Thus, in this study, HVOF was critically evaluated for the deposition of nickel-graphite coatings for applications in tribological interfaces. In addition, the microstructural, mechanical, and tribological behavior of the nickel graphite coatings with two different compositions (75Ni-25Gr and 85Ni-15Gr) was investigated in detail. Overall higher coating density was obtained with lower amounts of oxide and higher hardness in this study. The results showed that the friction coefficient for both coatings differ at tested temperatures, and overall, the value was higher at 450°C compared to the value at room temperature The specific wear rates however, showed little difference at room temperature, while the 75Ni-25Gr coating had a lower wear rate at elevated temperatures compared to 85Ni-15Gr. SEM analysis of the wear tracks and counterparts revealed the associated wear mechanisms. This study demonstrates the potential of HVOF for producing high-quality wear-resistant coatings and provides insights into the behavior of nickel-graphite coatings under different conditions, which can be useful for designing materials for demanding tribological applications.

Keywords: Nickel-Graphite coating, HVOF, Friction, Wear

3.2 Introduction

Engineered surfaces play a critical role in the performance and functionality of materials and components in gas turbine engines. In particular, the components must withstand critical challenges such as abrasive wear, corrosion, and erosion under high temperature and pressure conditions [1-4]. Such events can seriously impair the tribological functionality and service life of the component, which may result in component failure and destruction. Tribological coatings are widely used to enhance the performance of the substrate without altering the microstructure of the bulk material by changing the surface characteristics of the engineering part. Thermal spray processes can be used to develop many types of coatings, including ceramic, metal, cermet, and composite surfaces, and to repair worn and damaged parts to better than new condition [5,6]. Coatings developed by thermal spray have a lower environmental impact than alternatives such as electroplating and physical vapor deposition due to reduced material waste, reduced use of hazardous chemicals, and reclaimed coating material. In addition, they provide greater part longevity, reducing maintenance and required repair cycles [7-9]. In particular, plasma spraying, high velocity oxy-fuel (HVOF) and flame spraying techniques are commonly used in the aerospace industry [10-13], mostly for thermal barrier coatings and tribological applications. Among these techniques, HVOF is capable of producing damage-tolerant and wear resistant coatings thanks to two key characteristics of this process that are higher gas jet velocity and lower flame temperature. The higher gas jet velocity can be beneficial as the particles would impact the substrate with greater momentum, leading to coatings with improved adhesion to the substrate and improved cohesive strength between deposited particle splats. In addition, the lower flame temperature allows for reduced oxide levels compared to air plasma spraying. Other important properties of HVOF coatings include smooth, dense, high hardness coatings with homogeneous chemistry that require less post-treatment [14,15].

Ni-based thermal sprayed coatings have demonstrated effectiveness in corrosion, oxidation, and wear applications [16,17]. For example, Oksa et al. [19] observed that HVOF sprayed Ni-based coatings exhibited excellent corrosion resistance. Recently, to evaluate the wear performance of nickel-phosphorus coated powders for diverse applications, Mathiyalagan et. al [20] utilized High Velocity Air Fuel (HVAF) and took advantage of two different nozzle configurations to apply colder and hotter spraying conditions for the first time. The authors showed that the coefficient of

friction and specific wear rate were lower for the coating sprayed under hotter conditions. Nanocrystalline Ni-Al HVOF sprayed powder was also evaluated by several characterization techniques in a study by Enayati et al. [21]. The authors reported that the deposited coatings had excellent homogeneity and uniformity with low porosity and excellent contact with the substrate. The above research demonstrates the promising properties of Ni-based HVOF and HVAF sprayed coatings for various applications.

To reduce the coefficient of friction, Ni graphite (Ni-Gr) has been extensively investigated as an abradable coating in previous research [22-27]. The use of Ni-Graphite composite coatings to reduce fretting wear was also investigated by Hager et al. [28] who discovered that nickel graphite APS coatings reduced wear on mated Ti6Al4V surfaces at room temperature and 450 °C. The effect of APS on the wear behavior of Ni-Graphite coatings at elevated temperatures was investigated by Soltani et al. [29]. The authors identified the optimal process parameters, in particular hydrogen flow rate and spraying distance, to improve the abradability of this coating. The influence of graphite size and distribution on the friction and wear behavior of Ni-graphite coatings deposited by APS and supersonic APS (SAPS) techniques was investigated by Tang et al. [30]. Their results showed that SAPS provided higher wear resistance due to higher hardness and bond strength of the coating. The authors correlated the wear performance of the SAPS coating with higher in-flight velocity, which could reduce the degree of oxidation of Ni and also increase the hardness of the coating. In addition, the average size of the graphite phase was smaller in the SAPS coating than in the APS, which in turn would improve the formation of a graphitic tribofilm during sliding. These advantages are typical of those brought by HVOF; however, few studies have investigated the tribological characteristics of HVOF deposited Ni-Graphite coatings used as tribological interfaces. Therefore, the objective of this study is to investigate the effect of the HVOF deposition technique on the coating microstructure and reciprocating wear behavior of Ni-Graphite coatings with different compositions. The microstructure and hardness were investigated and the tribological properties of the as-received Ni-Graphite coatings were evaluated both at room and elevated temperature.

3.3 Experimental Methods

3.3.1 Materials and coating preparation

Commercially available Ni-Graphite powders were used as feedstock powders in this study: the powders were made of encapsulated graphite inside a nickel shell, with weight proportions of 75Ni-25Gr and 85Ni-15Gr (Metco 307NS-2 & Metco 308NS-1, Oerlikon Metco, Canada) and with a particle size range of - 90 + 30 μm. These powders are high purity powders (~99%). Low carbon steel with dimensions 1"×1"×0.17" (25.4mm × 25.4mm × 4.3mm) were used as substrate materials. The steel substrate surfaces were grit-blasted using 20-grit alumina abrasive particles to increase the surface roughness and improve adherence of the coatings to the substrates. Prior to coating deposition, the substrate was preheated to 150 °C while the maximum temperature of the substrates surface was maintained approximately at 135 °C during spraying. Ni-Graphite coatings were deposited on the grit-blasted substrates via HVOF (Oerlikon-Metco Diamond JetTM 2700 Gun, USA) and the deposition parameters are tabulated in Table 3.1. To decrease particle-flame interaction time and in-flight Ni oxidation during the spray process, the spraying parameters of pure Ni were chosen for HVOF deposition of Ni-Graphite coatings. The particle in-flight temperature and velocity were monitored using Accuraspray (Tecnar, Quebec, Canada) for both powders.

Table 3. 1 HVOF parameters

Parameters	Values	
	75Ni-25Gr	85Ni-15Gr
Gun transverse speed (mm/s)	1000	
Feed rate (g/min)	25	
Propylene flow rate (l/min)	75	
Oxygen flow rate (l/min)	165	
Air flow rate (l/min)	473	
Spraying distance (mm)	250	
Number of passes	20	
Substrate mean temperature (°C)	135	
In-flight particles temperature (°C)	1842	1492
In-flight particles velocity (m/s)	573	514

3.3.2 Microstructural characterization of coatings and worn surfaces

The microstructure and chemical composition of the as-sprayed coatings, as well as the wear tracks, were characterized by a field emission scanning electron microscope (FE-SEM) (SU8230, Hitachi, Japan) built with energy dispersive spectroscopy (EDS). Cross-sections were also prepared as per the standard on metallographic preparation (ASTM E03) (31). The graphite phase content as well as the porosity in both coatings were also measured by quantitative image analysis from 10 images with the same magnifications. It should be noted that porosities and graphite phase both looked pitch black and we tried to separate them with thresholding. The coating thicknesses were evaluated from the obtained cross-section images. The average coating thickness was determined from 10 images with the same magnifications, and standard mean error was reported. X-Ray Diffraction analysis (XRD) (X'pert, Malvern Panalytical, UK) was performed using a copper source (Cu Kα radiation, $\lambda = 1.5406$ Å) with a scan rate of 2 deg/min. Microhardness tests were performed using a Vickers microhardness tester (Anton Paar Micro Combi Tester, MCT3, Switzerland) at RT, on polished coating cross sections. A 1000 mN load with a dwell period of 10 seconds was employed to generate at least 10 indentations ($n = 10$) on both coatings. The average microhardness value with its standard deviation was reported in each case.

3.3.3 Wear tests

Dry wear tests were performed on the as-sprayed coatings using a ball-on-flat reciprocating tribometer (Anton Paar TriTec SA, Switzerland). Prior to testing, the surface roughness was analyzed using confocal laser microscope (Olympus LEXT 4000, USA), which was approximately 25 ± 5 µm for both coatings. A 6.35 mm alumina (Al_2O_3) ball was used as a counter body against the as-sprayed Ni-Graphite coatings. This was performed to understand the performance of the coating without any surface finishing processes, which would help reduce the lead time and overall component cost. Furthermore, Al_2O_3 was chosen as a counter body due to its high hardness and high thermal stability at elevated temperatures. Table 3.2 shows the parameters of the wear test. The testing was employed at two temperature conditions, room temperature (RT) and 450 °C. SEM and EDS were employed to determine the wear surface morphologies and identify the eventual formation of a mechanically mixed layer (MML) from top-surface and cross-section observation of the wear tracks. It should also be noted that gold was used as a conductive coat in the SEM

analysis. The counter body surfaces were also analyzed after the testing to determine the eventual formation of a transfer film.

Table 3. 2 Ball-on-flat reciprocating wear test parameters

Parameter	Values
Applied load (N)	5
Frequency (Hz)	1
Stroke length (mm)	10
Sliding velocity (cm/s)	3.14
Number of cycles	5000
Total sliding distance (m)	100
Counter ball diameter (mm)	6.35 (Alumina ball)

3.4 Results

3.4.1 Microstructure, characterization, and microhardness

The cross-sections of both sprayed Ni-Graphite coatings are presented in Fig. 3.1 a-d. The SEM elemental maps of the cross sections are also presented in Fig. 3.1. The thickness of the 75Ni-25Gr and 85Ni-15Gr coatings were measured to be 450 ± 21 μm and 360 ± 33 μm, respectively (see Fig. 3.1a and 3.1c). Deposition efficiency of the HVOF spraying process for 75Ni-25Gr and 85Ni-15Gr were also 70% and 47%, respectively. Both coating cross-sections (Fig. 3.1a and 3.1c) exhibit a homogenous and dense structure. The coating structure seems quite lamellar as can be seen by flattened splats at higher magnification (Fig. 3.1d). The coatings are comprised of light (nickel) and dark (graphite) areas (Fig. 3.1b) without any crack or delamination: these were determined to be nickel and graphite phases, respectively, by EDS. The EDS mapping (Fig. 3.1b and 3.1d) also shows quite low oxygen content in both coatings. The surface roughness (S_a) of both as-deposited coatings was also 23 ± 2.1 μm and 30 ± 4.6 μm for the 75Ni-25Gr and 85Ni-15Gr coatings, respectively. As is observed from Table 1, particle velocities and temperatures are relatively higher for the 75Ni-25Gr coating (573 m/s and 1842 °C) as compared to the 85Ni-15Gr coating (514 m/s and 1492 °C). Additionally, there are no obvious cracks and pores in nickel and graphite interfaces from SEM analysis, showing proper interfacial compatibility between the two elements during HVOF deposition.

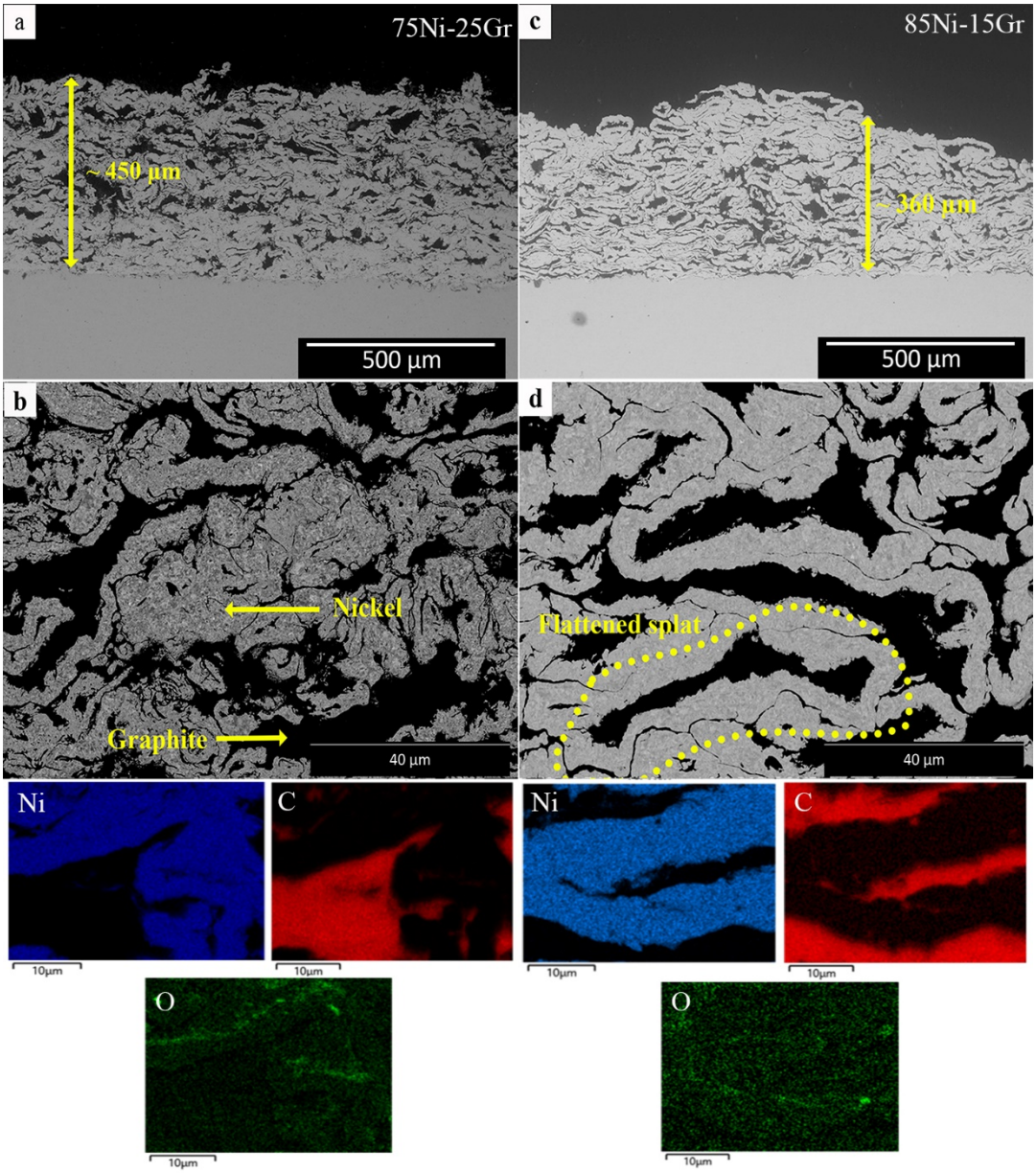

Figure 3. 1 Cross-section SEM images and elemental map analysis of both coatings: (a, b) 75Ni-25Gr, (c, d) 85Ni-15Gr.

The XRD patterns of the as-sprayed 75Ni-25Gr and 85Ni-15Gr HVOF coatings are presented in Fig. 3.2. In both coatings, diffraction peaks of nickel and graphite appeared, while no peak for oxygen was detected, meaning that oxide inclusion content was below the detection limit of the XRD machine (< 4%). This, in turn, can be interpreted by the fact that HVOF leads to less oxidation compared to its alternative technique, APS, due to operating at lower temperatures. As

mentioned, these results are in agreement with elemental mapping of the coatings (Fig. 3.1), indicating a low amount of oxygen in both coatings.

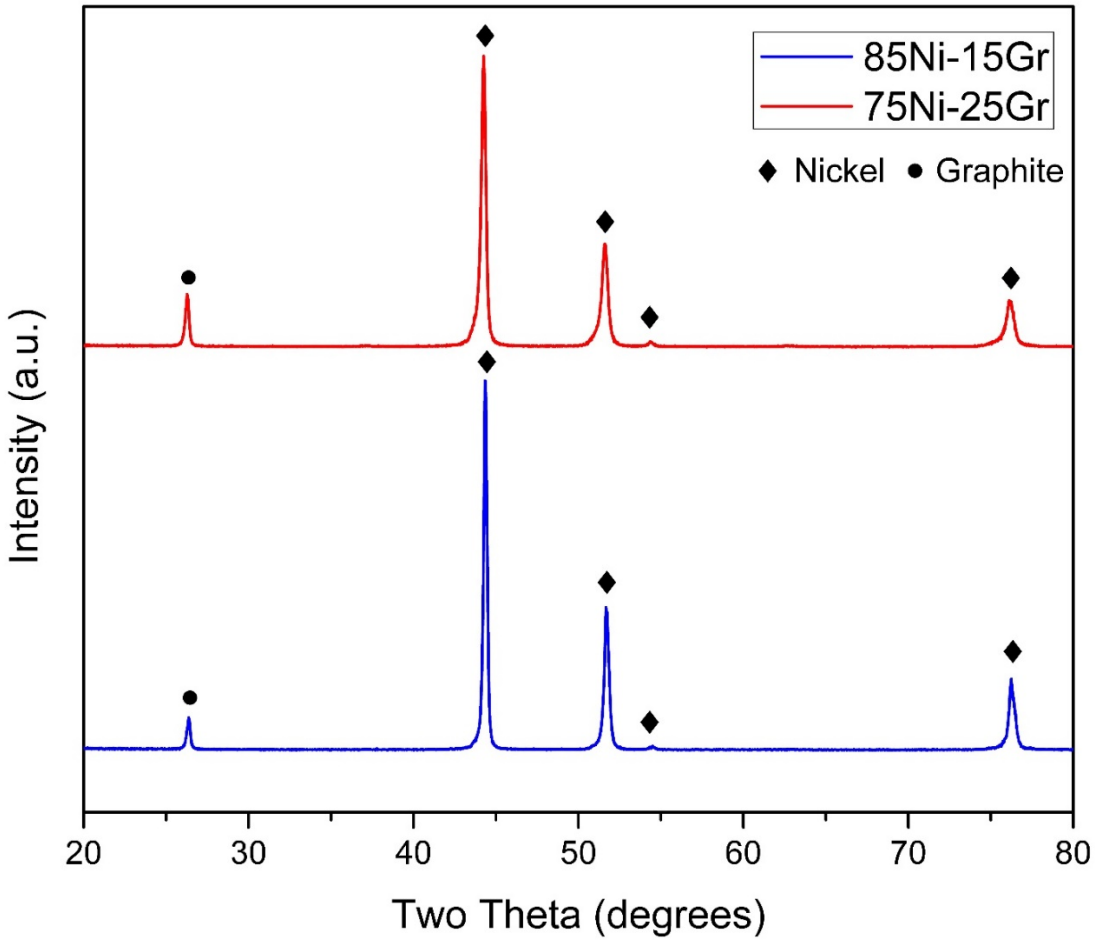

Figure 3. 2 XRD patterns of the 75Ni-25Gr and 85Ni-15Gr coatings

Several of the coating characteristics are listed in Table 3.3. The 85Ni-15Gr coating has an average microhardness value of 61 ± 13 $HV_{0.3}$, which is 40% higher than that of the 75Ni-25Gr coating with an average microhardness value of 43 ± 9 $HV_{0.3}$. The results from two-dimensional images illustrate that the graphite phase contents for 75Ni-25Gr and 85Ni-15Gr coatings were 30 ± 2.1% and 18 ± 1.3%, respectively. Based on the graphite volume percent in the coatings - 57% and 41% -, it could be concluded that 52% and 44% of the graphite was lost during spraying for 75Ni-25Gr and 85Ni-15Gr coatings, respectively.

Table 3. 3 Characteristics of 75Ni-25Gr and 85Ni-15Gr coatings

Coating	Thickness (µm)	Graphite content (%)	Porosity	Roughness (µm)	Microhardness (HV_1)
75Ni-25Gr	450 ± 21	30 ± 2.1	Less than 1%	23 ± 2.1	43 ± 9
85Ni-15Gr	360 ± 33	18 ± 1.3	Less than 1%	30 ± 4.6	61 ± 13

3.4.2 Friction and wear behaviors

The coefficient of friction as a function of the sliding cycles and test temperature is presented in Fig. 3.3. Both coatings illustrate friction-reducing performance with a short running-in regime in the first few cycles following a constant trend below 0.2 (steady state) until the end of the test at RT. These results are comparable to previously published literature on APS and cold sprayed Ni-Graphite coatings performed at RT [30-32]. At 450 °C, however, the friction coefficients show a different behavior, starting from a relatively low value (i.e. 0.2) and increasing moderately to approximately 0.4 after 1000 cycles. The coefficient of friction at the end of the test was approximately 0.45. The fluctuations of the friction curve at 450 °C was higher compared to the friction values at RT.

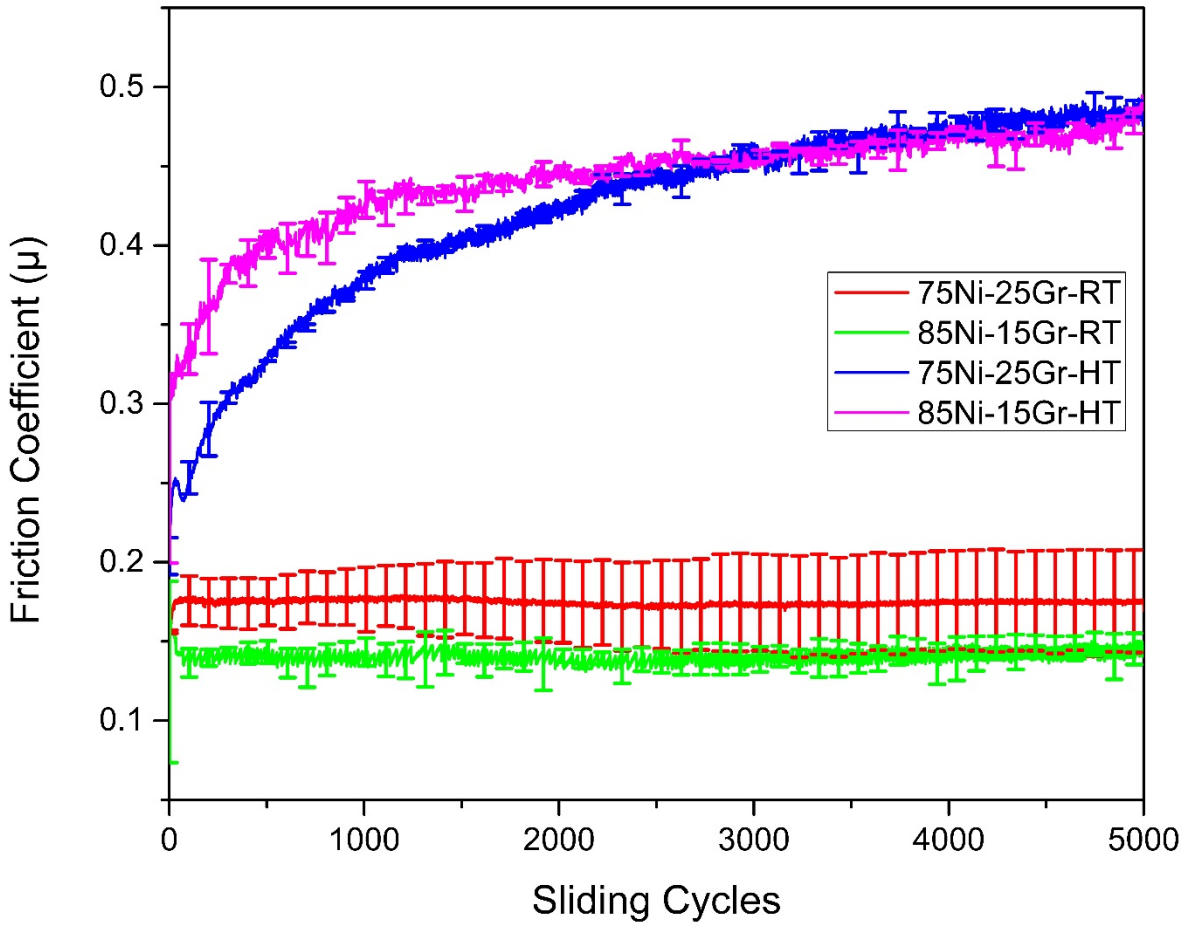

Figure 3. 3 Coefficient of friction of the 75Ni-25Gr and 85Ni-15Gr coatings at RT and 450 °C

Figure 3.4 shows the specific wear rates of the coatings. It can be observed that both coatings have relatively low wear rates at RT with a negligible difference, whereas at 450 °C, the wear rate increases drastically for both coatings. In addition, the wear rate of the 75Ni-25Gr coating at 450 °C was 12.9×10^{-4} $mm^3/N.m$ which is 30% less than that of 85Ni-15Gr (19.3×10^{-4} $mm^3/N.m$.).

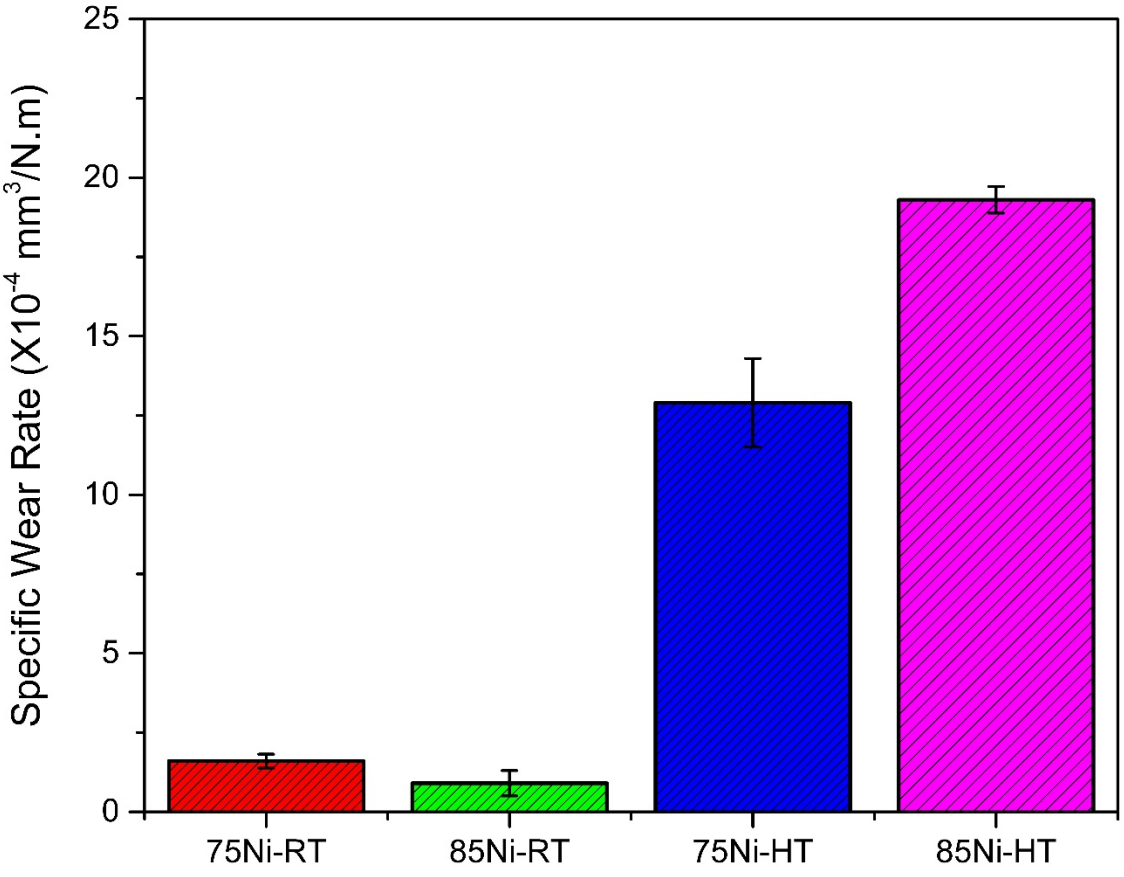

Figure 3. 4 Specific wear rate of the 75Ni-25Gr and 85Ni-15Gr coatings at RT and 450 °

Figure 3.5 shows the SEM images of the worn coating surfaces at RT. While the worn 75Ni-25Gr surface is mostly covered by smeared wear debris particles with more and wider cracks (Fig. 3.5a), the worn 85Ni-15Gr surface is comprised of a smoother and denser worn surface with smaller cracks (Fig. 3.5b). EDS color maps of the worn coating surfaces are also presented in Fig. 3.5. Interestingly, the worn 85Ni-15Gr surface shows more oxygen-rich areas corresponding to the formation of Ni oxides when compared to the worn 75Ni-25Gr surface.

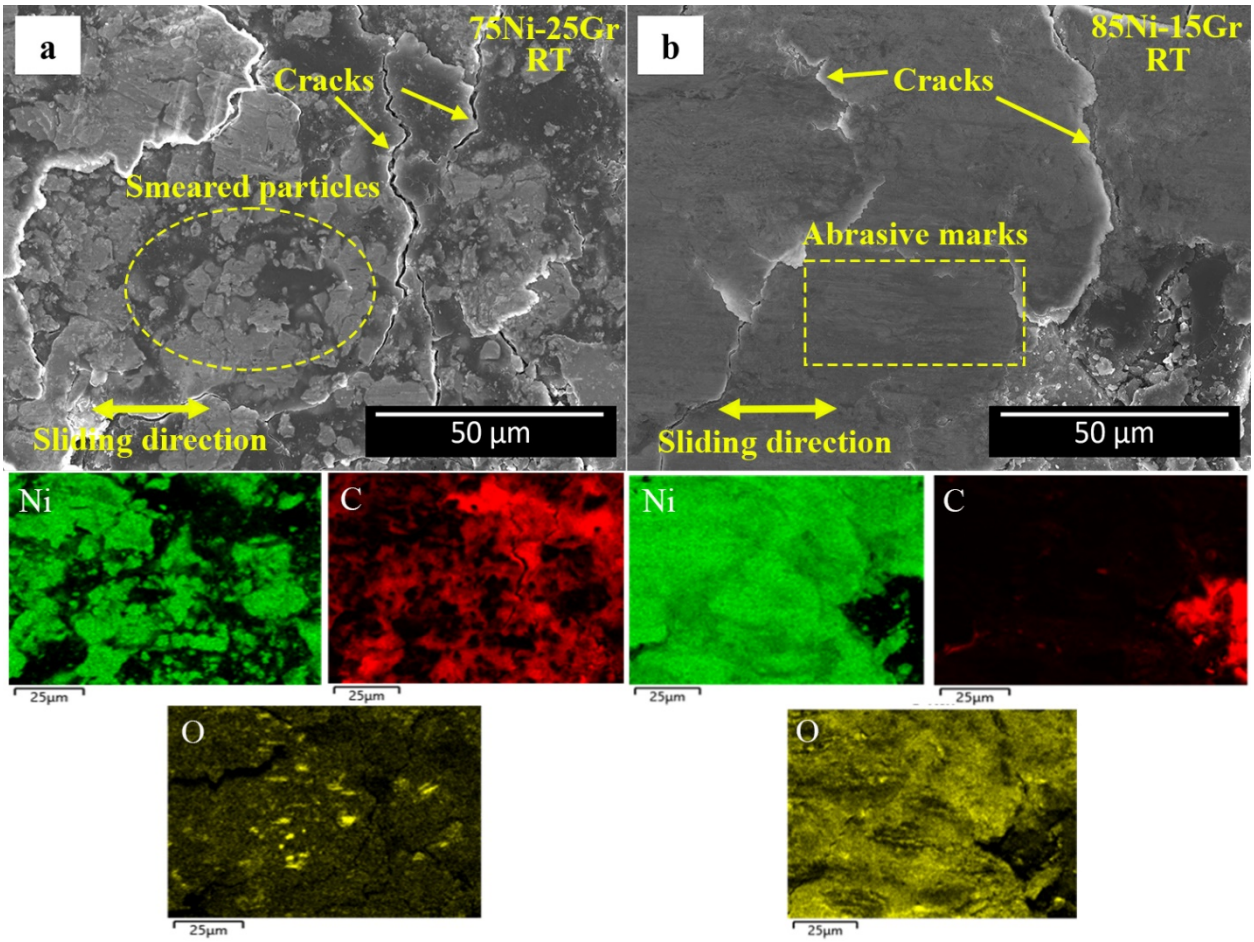

Figure 3. 5 Worn surface SEM images and elemental map analysis of the (a) 75Ni-25Gr and (b) 85Ni-15Gr coatings at RT

SEM images of the worn surfaces tested at 450 °C are illustrated in Figure 3.6. Also, they exhibited that the width and depth of the wear tracks at 450 °C were larger than at RT (not presented here). The worn surface of both coatings showed a smeared layer. In 75Ni-25Gr, the presence of pits and scratches parallel to sliding direction appeared throughout the worn surface (Fig. 3.6a) whereas the worn 85Ni-15Gr surface was mostly covered by fine cracks and more scratches (Fig. 3.6b). In addition, EDS characterization was also carried out for the worn sliding surfaces at 450 °C (also in Fig. 3.6) and the EDS mapping images showed that the worn surface of both coatings is enriched in oxygen, with lower amount of graphite content.

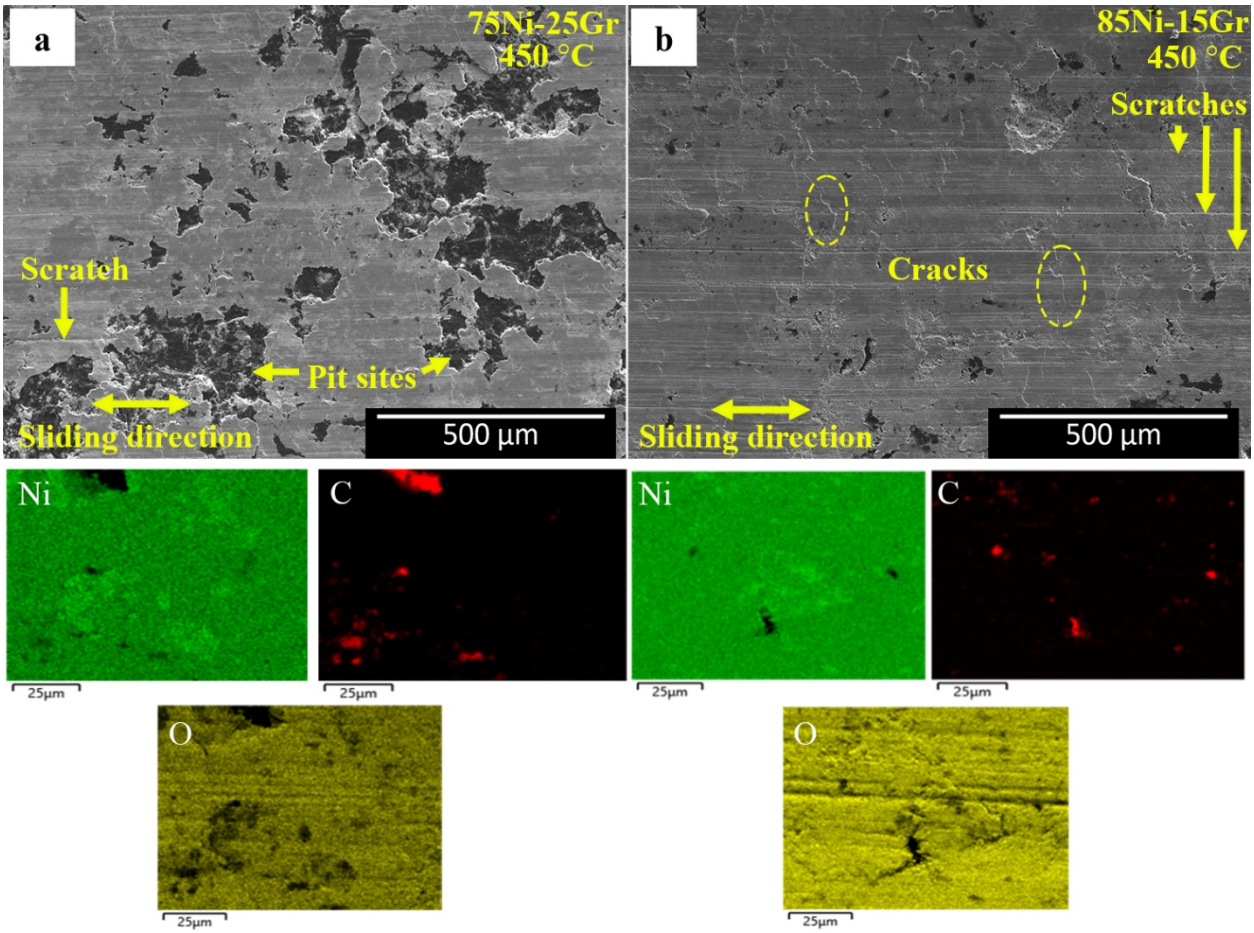

Figure 3. 6 Worn surface SEM images and elemental map analysis of the (a) 75Ni-25Gr and (b) 85Ni-15Gr coatings at 450 °C

Figure 3.7 shows cross-sectional micrographs of both worn coatings (i.e. 75Ni-25Gr and 85Ni-15Gr) at 450 °C. A thick MML was formed on both worn coating surfaces at high temperature (Fig. 3.7a and 3.7c). SEM images of the cross sections at higher magnification (Fig. 3.7b and 3.7d) showed that the thickness of the formed MML in 75Ni-25Gr coating (12 ± 3 µm) was 35% higher than that of 85Ni-15Gr (7 ± 2 µm). Additionally, more microcracks were observed in the 85Ni-15Gr MML as compared to 75Ni-25Gr. EDS characterization was also conducted for the formed MML, and the EDS area (Fig. 3.7e) and line scan analyses (Fig. 3.7f) imply the presence of nickel, graphite, and a high amount of oxygen in these regions. Trace amounts of aluminum were also found however, it was neglected in the final analysis. It should be noted that the presence of gold in the EDS spectrum of Fig. 3.7e is related to the conductive gold coat used for the SEM analysis, as mentioned in the Experimental Methods.

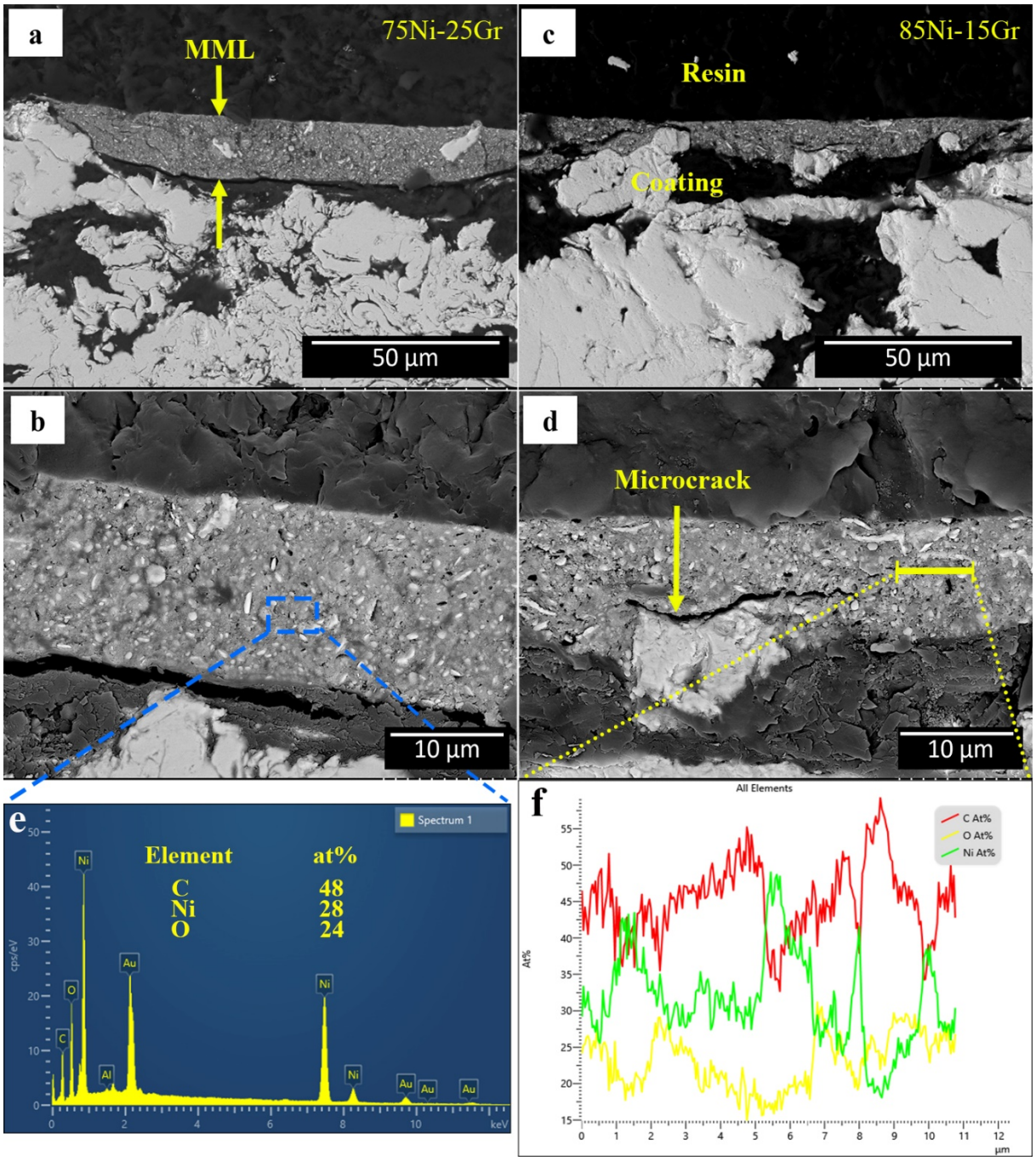

Figure 3. 7 SEM cross section images of the worn surfaces at 450 °C for both coatings:(a,b) 75Ni-25Gr,(c,d) 85Ni-15Gr.(e) and (f) are corresponding EDS results to (b) and (d)

The SEM micrographs of the alumina counter-balls after sliding against the coatings at RT and 450 °C are displayed in Fig. 3.8. Although no transfer film appeared on the counterparts at RT (Fig. 3.8a and 3.8b), a transfer film formed on the alumina counter balls at 450°C (Fig. 3.8c and

3.8d). These films contain mostly nickel and oxides as can be observed from the EDS results in Fig. 3.8c and 3.8d. The counterfaces from the wear tests performed at RT show the lowest amount of scratches parallel to the sliding direction with some presence of graphite debris (see Fig. 3.8a and 3.8b).

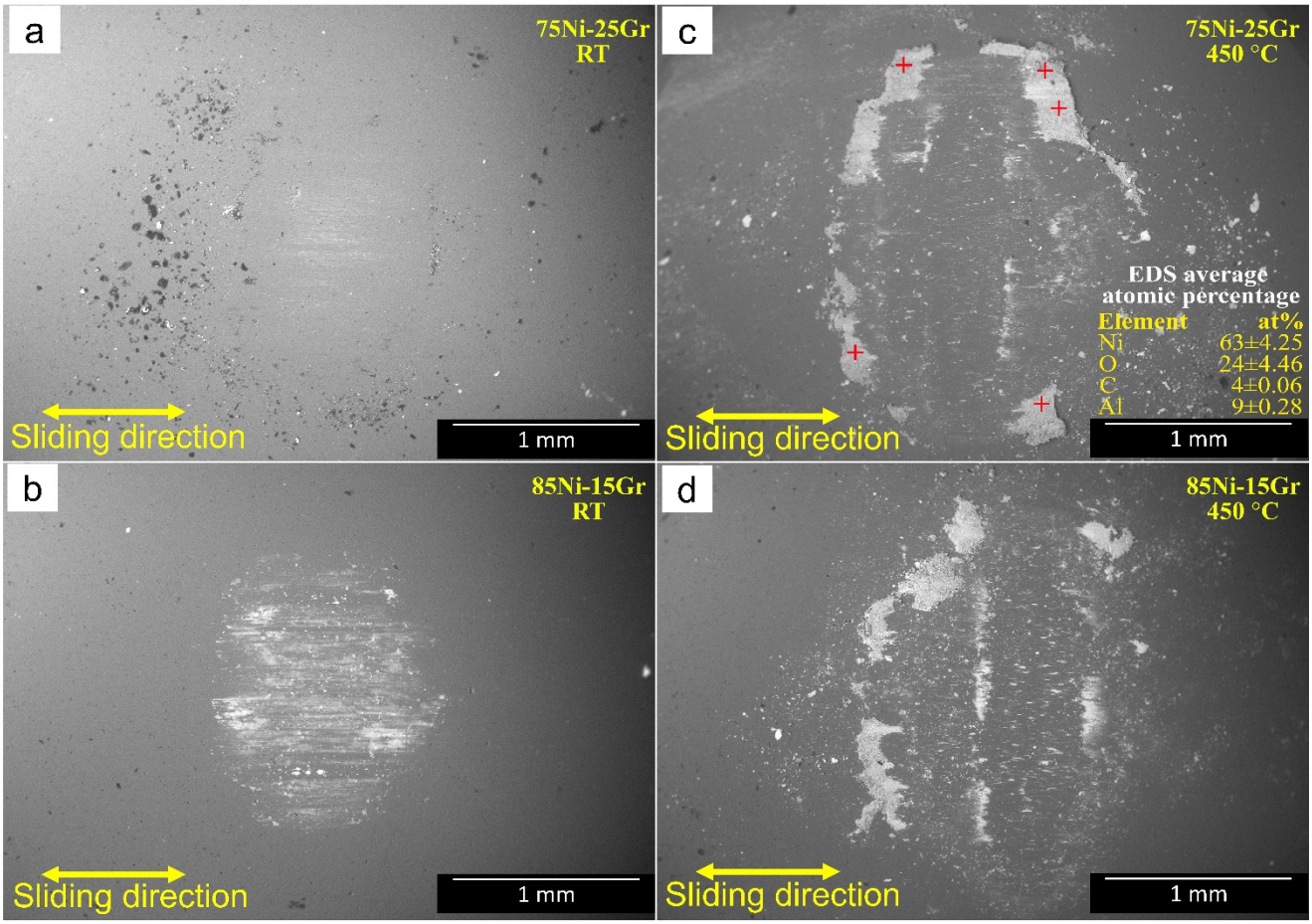

Figure 3. 8 SEM images of the alumina counter-balls sliding against Ni-Gr coatings at different temperatures: (a and b) at RT and (c and d) at 450°C.

3.5 Discussion

3.5.1 Microstructure, characterization, and microhardness

Based on the coating cross-section micrographs shown in Fig. 3.1, thermally sprayed Ni-Graphite splats remained un-molten and plastically deformed during HVOF spraying (Fig. 3.1d). The as-sprayed particles within the coatings (Fig. 3.1d) are similar to that of single flattened Ni-Graphite particle's shape observed in literature [27]. As shown in Table 3.1, particle velocities are

relatively high with HVOF compared to conventional APS, and particle temperatures are low, close to the melting point of nickel (1455 ºC). Therefore, while the powders may have passed a high-temperature flame region during the supersonic speed propulsion process, they did not have enough time to melt. Consequently, powders could not reach the melting temperature of nickel and appear as un-melted particles in the final deposits. In addition, the presence of low oxide inclusion content in the coatings seems to be due to the quick processing time in HVOF, which reduces the amount of time that the stream of molten or semi-molten particles interacts with the environment [33]. As a result, less in-flight exposure time helps reduce the degradation of the initial powder feedstocks. The XRD results (Fig. 3.2) directly support this idea as it does not show any oxygen contents in both coatings. These results are in agreement with the results from color mapping analysis (Fig. 3.1), proving the presence of little amount of oxygen in the coatings. Somervuori et. al. reported no visible oxide clusters or bands in HVOF deposited Ni-based coating in comparison with APS [34].

Nickel as the metallic matrix (bright area in Fig. 3.1b), encapsulates the graphite particles as a shell (dark area in Fig. 3.1b) increasing the bonding strength and hardness of the coating. Consequently, this resulted in a dense coating with a low amount of porosity (less than 1%) (Table 3.3). The results obtained from the Vickers microhardness measurements (Table 3.3) indicate that the 85Ni-15Gr coating is harder than the corresponding 75Ni-25Gr coating. The higher hardness of 85Ni-15Gr coating can be explained by the higher content of nickel in this coating. This is consistent with prior work by Hamed et. al. who also found higher hardness in Ni-based wear resistant plasma sprayed coatings with higher amounts of nickel [35].

3.5.2 Friction and wear behavior

The friction coefficient of the Ni-Graphite coatings was between 0.10 and 0.20 at RT (Fig. 3.3) which was consistent with the study conducted by Hager et al. (28), who showed that the friction value of Ni-Graphite coatings deposited by APS was ~0.3 when tested at RT. Soltani et al. also [29] reported similar friction behavior for Ni-Graphite powders coated by APS. Interestingly however, the friction coefficient of HVOF sprayed Ni-Graphite coatings at RT in our study was lower both in running-in and steady state stages. Also, similar to what was concluded from literature [28], compositions of 15% and 25% graphite in the pre-spray powder mixture had similar

effectiveness in decreasing the friction between the Ni-based HVOF sprayed coatings and the mated alumina balls. Therefore, it is likely that a higher amount of entrapped particles generated on the worn 75Ni-25Gr surface (Fig. 3.5a) could have resulted in a further increase of the friction values compared to 85Ni-15Gr coating, which is comprised of a smoother surface with less wear debris particles (Fig. 3.5b). Although more lubricating graphite-based tribofilm could exist on frictional surface of 75Ni-25Gr coating compared to 85Ni-15Gr (Fig. 3.5) it is not completely intact in combination of wear debris. These wear debris then act as two or three body particles during sliding causing the friction increase for 75Ni-25Gr compared to 85Ni-15Gr [36].

At 450 °C, the friction coefficient of the Ni-Graphite coatings was notably higher (Fig. 3.3). This is consistent with the behavior observed for Ni-Graphite coatings produced by APS when tested at 450 °C by Hager et al. [28]. The increment of the friction coefficient can be explained by the poor lubrication properties of graphite based on the lower amounts of water vapor [37] and oxidation of coating materials at elevated temperatures. Thus, throughout the initial wear cycles, the direct ceramic-on-ceramic (alumina-on-NiO) contact would cause high tangential stresses at the sliding surfaces. Consequently, shearing/ fracture of oxidized (NiO) asperities lead to the generation of wear debris of oxide particles [38]. It is likely that the wear debris particles get compacted to generate a thin NiO transfer layer. The higher friction coefficient value for 85Ni-15Gr coating at the initial stages of sliding (Fig. 3.3) can be correlated to the higher content of nickel and lower amount of graphite phase.

The wear rates at RT for both coatings followed the same trend, with relatively low volume loss compared to tests performed at 450 °C (Fig. 3.4). This can possibly be explained by the formation of a graphite-based tribofilm between the 75Ni-25Gr coating and mating material. Huang et al. showed that graphite had been squeezed out from the nickel shells and abraded to form a thin graphitic film on the surface during the sliding process [32]. Similarly, for the 85Ni-15Gr coating the wear rate was lower at RT when compared to that of the high temperature tests, which could be explained by the formation of an oxygen-rich layer on the worn surface (Fig. 3.5b). Soltani et al. also found that the generated frictional heat during sliding caused the surface temperature rise and hence oxidation of top layers of nickel splats to NiO . Indeed, formation of such an oxygen-rich layer on the surface (Fig. 3.5b) would contribute to the hardness enhancement and thus decreasing the wear rate of 85Ni-15Gr coatings at RT. Similarly, Torgerson et al. reported

that formed NiO (i.e. confirmed with Raman spectroscopy) on the cold sprayed nickel coating was responsible for friction coefficient and wear rate reduction at RT [40].

At elevated temperature, however, the wear rate increased significantly (Fig. 3.4). Based on the compositional analysis (Fig. 3.6a and b), the worn surface of both coatings was rich in oxygen. This is consistent with the SEM analysis of the worn surface cross-sections at 450 °C (Fig. 3.7e and 3.7f) revealing the presence of a thick MML on the worn surface of both coatings that is composed of high nickel and oxygen contents. In a similar study, Barrau et al. reported that the brittle oxidized particles could become entrapped between the sliding surfaces and get compacted due to the repetitive sliding and induced localized pressure and formed a thin MML over the surface. It is possible that the unstable and brittle nickel oxide layers at elevated temperature removed over the span of sliding and led to significant plastic flow and shear deformation of material causing the increase in both friction coefficient and wear volume loss (Fig. 3.3 and 3.4) [42]. Peterson et. al. conducted comprehensive research on sliding characteristic of various metals / oxides and observed that NiO has undesired friction coefficient at high temperature with the value of approximately 0.7 among other oxides. [43]. When comparing the formed MML at elevated temperature on the worn surfaces of the two coatings (Fig. 3.7b and 3.7d), it is noted that a thinner layer (7 ± 2 μm) has been formed on 85Ni-15Gr coating compared to 75Ni-25Gr (12 ± 3 μm). Microcracks are also present along the MML region of this coating (i.e. marked by arrow in Fig. 3.7d). It is possible that the thinner layer is less protective compared to the thicker layer (12 ± 3 μm) in the 75Ni-25Gr coating, which resulted in a higher volume loss with the 85Ni-15Gr coating. In addition, numerous grooves parallel to the sliding direction are present on the wear tracks of both coatings (Fig. 3.6a and 3.6b) at 450 °C, indicating that the governing wear mechanism was abrasion. The presence of abrasive oxide particles at the interface could have also contributed to the high wear rates at elevated temperature, especially for 85Ni-15Gr coating with high nickel content. EDS area analysis and line scan of the formed MML (Fig. 3.7e and 3.7f) showed high oxygen and nickel contents, confirming the presence of abrasive NiO particles on the surface.

Based on the above observations, the sliding wear mechanisms of Ni-Graphite HVOF coatings at RT and 450 °C can be proposed as shown in Fig. 3.9. At RT the lowest friction coefficient and wear rate for both coatings (Fig. 3.3 and 3.4) were seemingly governed by the formation of a continuous tribofilm (i.e. graphite based and oxide based). At 450 °C, the wear

mechanism is mainly the synergy of abrasive wear with oxidative nature and a higher friction coefficient for both coatings (Fig. 3.3). In addition, the formation of a MML caused higher friction coefficient and wear rate for both coatings at elevated temperature. The formation of a weak and unstable MML containing cracks (Fig. 3.7a-c) resulted in a significant transfer of mating materials to the alumina counter balls (Fig. 3.8b). MML with lesser microcracks compared to 85Ni-15Gr coating (Fig. 3.7b-d).

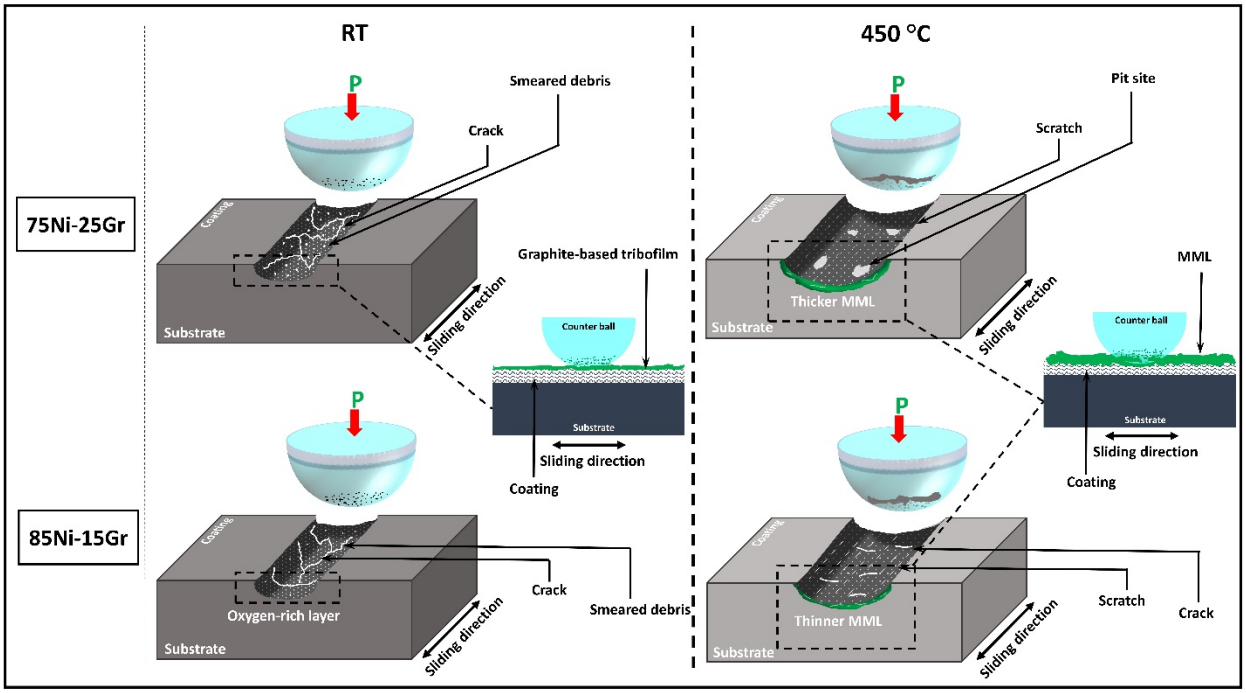

Figure 3. 9 Schematic of wear mechanisms of the Ni-Gr HVOF coatings at RT and 450 °C

3.6 Conclusion

Ni-Graphite coatings with different compositions were deposited on mild steel substrates by HVOF. The tribological behavior of as-sprayed coatings were investigated both at RT and 450 °C. In addition, the effect of the coating microstructure on the wear and friction behavior was discussed. The fully dense HVOF Ni-Graphite coatings with negligible amount of oxide possessed low friction coefficients with values of 0.2. More specifically, the formation of a graphite-based and oxygen-based tribofilm helped reduce the coefficient of friction and wear at RT. However, at elevated temperature (450 °C), the coefficient of friction and specific wear rate of both coatings

was substantially higher compared to RT. At 450 °C, the wear was dominated by abrasion with oxidative nature in both coatings. In addition, the formation of an MML at higher temperature led to a higher friction coefficient and specific wear rate. This was associated with the brittle nature of the formed nickel oxide at elevated temperature.

References:

1. Bruzzone AAG, Costa HL, Lonardo PM, Lucca DA. Advances in engineered surfaces for functional performance. CIRP Annals. 2008;57(2):750–69.

2. Barshilia HC. Surface Modification Technologies for Aerospace and Engineering Applications: Current Trends, Challenges and Future Prospects. Trans Indian Natl Acad Eng. 2021 Jun;6(2):173–88.

3. Xue YJ, Zhang YZ. Surface coatings in tribological and wearresistant applications. International Heat Treatment and Surface Engineering. 2009 Jun;3(1–2):17–25.

4. Yin S, Cizek J, Suo X, Li W, Liao H. Thermal Spray Technology. Advances in Materials Science and Engineering. 2019 Jan 9;2019:1–2.

5. Lince J. Coatings for Aerospace Applications. 2017 [cited 2022 Dec 21]; Available from: http://rgdoi.net/10.13140/RG.2.2.21638.16964

6. Hardwicke CU, Lau YC. Advances in Thermal Spray Coatings for Gas Turbines and Energy Generation: A Review. J Therm Spray Tech. 2013 Jun;22(5):564–76.

7. Pawlowski L. The Science and Engineering of Thermal Spray Coatings [Internet]. 1st ed. Wiley; 2008 [cited 2022 Dec 21]. Available from: https://onlinelibrary.wiley.com/doi/book/10.1002/9780470754085

8. Future Development of Thermal Spray Coatings [Internet]. Elsevier; 2015 [cited 2022 Dec 23]. Available from: https://linkinghub.elsevier.com/retrieve/pii/C2013016360X

9. Dowson D. Thinning films and tribological interfaces: proceedings of the 26th Leeds-Lyon Symposium on Tribology held in the Institute of Tribology, School of Mechanical Engineering, the University of Leeds, UK 14th-17th September, 1999. Amsterdam: Elsevier Science; 2000.

10. Krishna Upadhyay R, Annamalai Kumaraswamidhas L. A Review On Tribology Of Surfaces And Interfaces. Adv Mater Lett. 2014 Sep 1;5(9):486–95.

11. Matthews A, Franklin S, Holmberg K. Tribological coatings: contact mechanisms and selection. J Phys D: Appl Phys. 2007 Sep 21;40(18):5463–75.

12. Holmberg K, Matthews A. Coatings tribology: properties, mechanisms, techniques and applications in surface engineering. 2nd ed. Amsterdam ; Boston: Elsevier Science; 2009. 560 p. (Tribology and interface engineering series).

13. Kesavan D, Kamaraj M. The microstructure and high temperature wear performance of a nickel base hardfaced coating. Surface and Coatings Technology. 2010 Sep;204(24):4034–43.

14. Pauzi AA, Ghazali MJ, W. Zamri WFH, Rajabi A. Wear Characteristics of Superalloy and Hardface Coatings in Gas Turbine Applications–A Review. Metals. 2020 Sep 1;10(9):1171.

15. ASM Thermal Spray Society. Thermal Spray Processes and Application Examples. In: ASM Thermal Spray Society, editor. Thermal Spray Technology [Internet]. ASM International; 2022 [cited 2022 Dec 24]. p. 10–9. Available from: https://dl.asminternational.org/handbooks/book/181/chapter/3673014/Thermal-Spray-Processes-and-Application-Examples

16. Yu J, Wang Y, Zhao X, Li Q, Qiao Q, Zhao J, et al. Wear Resistance of Ni-Based Alloy Coatings. Advances in Materials Science and Engineering. 2019 Jul 30;2019:1–7.

17. Pomeroy MJ. Coatings for gas turbine materials and long term stability issues. Materials & Design. 2005 May;26(3):223–31.

18. Jha M, Kumar D, Singh P, Walia RS, Murtaza Q. Characterization of Ni-Based Alloy Coating by Thermal Spraying Process. In: Singari RM, Mathiyazhagan K, Kumar H, editors. Advances in Manufacturing and Industrial Engineering [Internet]. Singapore: Springer Singapore; 2021 [cited 2022 Dec 24]. p. 825–34. (Lecture Notes in Mechanical Engineering). Available from: http://link.springer.com/10.1007/978-981-15-8542-5_72

19. Oksa M, Auerkari P, Salonen J, Varis T. Nickel-based HVOF coatings promoting high temperature corrosion resistance of biomass-fired power plant boilers. Fuel Processing Technology. 2014 Sep;125:236–45.

20. Mathiyalagan S, Rossetti M, Björklund S, Sowers S, Dumm T, Kim C, et al. High velocity air fuel (HVAF) spraying of nickel phosphorus-coated cubic-boron nitride powders for realizing high-performance tribological coatings. Journal of Materials Research and Technology. 2022 May;18:59–74.

21. Enayati MH, Karimzadeh F, Tavoosi M, Movahedi B, Tahvilian A. Nanocrystalline NiAl Coating Prepared by HVOF Thermal Spraying. J Therm Spray Tech. 2011 Mar;20(3):440–6.

22. Song SP, Li C, Ji ZH. Orthogonal Analysis on Hardness of Nickel/Graphite Sealing Coating. AMM. 2012 Apr;164:55–8.

23. Xue W, Gao S, Duan D, Wang L, Liu Y, Li S. Study on the High-Speed Rubbing Wear Behavior Between Ti6Al4V Blade and Nickel–Graphite Abradable Seal Coating. Journal of Tribology. 2017 Mar 1;139(2):021604.

24. Ma X, Matthews A. Evaluation of abradable seal coating mechanical properties. Wear. 2009 Sep;267(9–10):1501–10.

25. Dadouche A, Conlon MJ, Dmochowski W, Liko B, Bedard JP. Experimental Evaluation of Abradable Seal Performance at High Temperature. In: Volume 5: Structures and Dynamics, Parts A and B [Internet]. Berlin, Germany: ASMEDC; 2008 [cited 2023 Jan 25]. p. 143–50. Available from: https://asmedigitalcollection.asme.org/GT/proceedings/GT2008/43154/143/324605

26. Gao S, Xue W, Duan D, Li S. Tribological behaviors of turbofan seal couples from friction heat perspective under high-speed rubbing condition. Friction. 2016 Jun;4(2):176–90.

27. Ziegelheim J, Lombardi L, Cesanek Z, Houdkova S, Schubert J, Jech D, et al. Abradable Coatings for Small Turboprop Engines: A Case Study of Nickel-Graphite Coating. J Therm Spray Tech. 2019 Apr;28(4):794–802.

28. Hager CH, Sanders J, Sharma S, Voevodin AA. The use of nickel graphite composite coatings for the mitigation of gross slip fretting wear on Ti6Al4V interfaces. Wear. 2009 Sep;267(9–10):1470–81.

29. Soltani R, Heydarzadeh-Sohi M, Ansari M, Afsari F, Valefi Z. Effect of APS process parameters on high-temperature wear behavior of nickel–graphite abradable seal coatings. Surface and Coatings Technology. 2017 Jul;321:403–8.

30. Tang JJ, Liu K, Yang QZ, Wang YH, Zhang P, Wang Y, et al. The influence of size and distribution of graphite on the friction and wear behavior of Ni–graphite coatings. Surface and Coatings Technology. 2014 Aug;252:48–55.

31. E04 Committee. Guide for Preparation of Metallographic Specimens [Internet]. ASTM International; [cited 2023 Feb 18]. Available from: http://www.astm.org/cgi-bin/resolver.cgi?E3-11R17

32. Huang C, Li W, Xie Y, Planche MP, Liao H, Montavon G. Effect of Substrate Type on Deposition Behavior and Wear Performance of Ni-Coated Graphite/Al Composite Coatings Deposited by Cold Spraying. Journal of Materials Science & Technology. 2017 Apr;33(4):338–46.

33. El-Eskandarany MS. Utilization of ball-milled powders for surface protective coating. In: Mechanical Alloying [Internet]. Elsevier; 2020 [cited 2023 Jan 24]. p. 309–34. Available from: https://linkinghub.elsevier.com/retrieve/pii/B9780128181805000121

34. Somervuori M, Varis T, Oksa M, Suhonen T, Vuoristo P. Comparative Study on the Corrosion Performance of APS-, HVOF-, and HVAF-Sprayed NiCr and NiCrBSi Coatings in NaCl Solutions. J Therm Spray Tech. 2022 Jun;31(5):1581–97.

35. Hamed K, El-Mahallawy N, Mokhtar MOA. An investigation of plasma sprayed nickel-based and pure aluminum coatings on austenitic stainless steel AISI 304. IOP Conf Ser: Mater Sci Eng. 2021 Aug 1;1172(1):012025.

36. Abrasive, Erosive and Cavitation Wear. In: Engineering Tribology [Internet]. Elsevier; 2014 [cited 2023 Feb 10]. p. 525–76. Available from: https://linkinghub.elsevier.com/retrieve/pii/B9780123970473000114

37. Bryant PJ, Gutshall PL, Taylor LH. A study of mechanisms of graphite friction and wear. Wear. 1964 Jan;7(1):118–26.

38. Fundamentals of Contact Between Solids. In: Engineering Tribology [Internet]. Elsevier; 2014 [cited 2023 Jan 24]. p. 475–524. Available from: https://linkinghub.elsevier.com/retrieve/pii/B9780123970473000102

39. Bidmeshki C, Abouei V, Saghafian H, Shabestari SG, Noghani MT. Effect of Mn addition on Fe-rich intermetallics morphology and dry sliding wear investigation of hypereutectic Al-17.5%Si alloys. Journal of Materials Research and Technology. 2016 Jul;5(3):250–8.

40. Torgerson TB, Harris MD, Alidokht SA, Scharf TW, Aouadi SM, Chromik RR, et al. Room and elevated temperature sliding wear behavior of cold sprayed Ni-WC composite coatings. Surface and Coatings Technology. 2018 Sep;350:136–45.

41. Liu Q, Castillo-Rodríguez M, Galisteo A, Guzmán de Villoria R, Torralba J. Wear Behavior of Copper–Graphite Composites Processed by Field-Assisted Hot Pressing. J Compos Sci. 2019 Mar 25;3(1):29.

42. Barrau O, Boher C, Gras R, Rezai-Aria F. Wear mecahnisms and wear rate in a high temperature dry friction of AISI H11 tool steel: Influence of debris circulation. Wear. 2007 Sep;263(1–6):160–8.

43. Peterson MB, Florek JJ, Lee RE. Sliding Characteristics of Metals at High Temperatures. A S L E Transactions. 1960 Jan;3(1):101–9.

44. Munagala VNV, Alidokht SA, Sharifi N, Makowiec ME, Stoyanov P, Moreau C, et al. Room and elevated temperature sliding wear of high velocity oxy-fuel sprayed Diamalloy3001 coatings. Tribology International. 2023 Feb;178:108069.

Chapter

4. MICROSTRUCTURAL, MECHANICAL, AND TRIBOLOGICAL EVALUATION OF CUAL-BASED COATINGS DEPOSITED BY APS AND HVOF

In this chapter…

The tribological studies between the atmospheric plasma spray and high velocity oxy-fuel Cu-Al have been provided. The testing, characterization and data analysis was performed to understand the friction and wear behavior at varying temperatures.

4.1 Abstract

Thermal-sprayed coatings have been extensively used in aerospace with the main purpose to overcome critical challenges such as abrasive wear, corrosion, and erosion under high temperatures and pressures. Such protective coatings can also play a crucial role in optimizing the efficiency of gas turbine engines and therefore in reducing fuel consumption and CO_2 emissions. CuAl-based thermal sprayed coatings are commonly employed in tribological interfaces within gas turbine engines to improve the wear resistance. These coatings are typically deposited by more traditional thermal spray technique such as Air Plasma Spray (APS), which can result in high amounts of oxidation within the coating. The main purpose of this study is to critically evaluate lower temperature deposition technique such as High Velocity Oxygen Fuel (HVOF). More specifically, commercially available Cu-10Al powders were deposited by APS and HVOF and compared in terms of their microstructural, mechanical properties, and tribological behavior at various temperatures. The results showed that the friction coefficient for both coatings was equivalent at room temperature while it was lower for the APS coating at high temperature when compared to the HVOF one. The specific wear rates showed difference between the different deposition processes at all temperatures.More specifically, the APS coating had a lower wear rate when compared to the HVOF coating. The differences in the friction and wear behavior were attributed to differences in the interfacial processes.

Keywords: APS, HVOF, Cu-Al, Wear, Friction

4.2 Introduction

The growing aero gas turbine market is confronted with significant technical challenges as their components operate in harsh and demanding environments (e.g., wide range of temperatures, high contact pressures, water vapor and solid particle erosion) [1–5]. Thus, there is a strong desire to develop durable, economically viable, and easy-to-implement new materials that can enhance the mechanical, physical, thermal, or chemical properties of the underlying substrate [6–10]. Notably, sliding aero engine parts undergo high friction and wear losses at their tribological interfaces. Such phenomena can significantly affect the performance and service life of the tribological system leading to fracture and devastation of tribo-components. To modify the surface characteristics of the engineering part without making any microstructural changes in the bulk material, tribological coatings are extensively applied to improve the substrate performance [11]. Surface coatings can lower the material loss and friction coefficient, where needed, by resisting various types of wear such as abrasive, adhesive, erosive, and cavitation [12].

Thermal spraying techniques have been increasingly used to apply advanced coatings of various nature (polymeric, metallic, ceramic) to lower surface roughness, improve corrosion and oxidation resistance, and protect the surface from wear and erosion [13]. Thermally sprayed coatings are more environmentally friendly and easy-to-implement with reduced environmental impact [14–16]. Consequently, excess bulk materials can be saved, and the component's life can be extended as well, thus reducing global warming by avoiding excessive materials usage and improving fuel efficiency. Compared to the energy-intensive processes such as melting, casting, extrusion, and welding, thermal spraying contributes significantly less to global warming [17]. Moreover, they offer much higher deposition rates with ranges from several micrometers to several millimeters or more, compared to alternative spraying processes such as electroplating and physical vapor deposition [18].

Among different types of spraying processes, Air Plasma Spraying (APS), High Velocity Oxy-Fuel (HVOF) and Flame Spraying (FS) are the most widely used techniques in the aerospace industry. More specifically, APS and HVOF are the most common techniques to produce tribological coatings employed for aerospace gas turbines [19]. The more traditional APS process sprays high-melting-temperature materials using ultra-high temperature plasmas and low gas jet velocity. Whereas HVOF can produce high quality coatings taking advantage of greater particle

impact velocity while operating at lower process temperatures than APS [20]. HVOF sprayed anti-abrasion coatings have become a promising alternative to APS-sprayed coatings, and higher densities, higher bond strengths, higher hardness and improved wear resistance have been reported [21].

Copper-based coatings have gained more attention to improve the wear and corrosion resistance of engineering parts in gas turbine engines and in the marine industry [22–25]. Thermally sprayed relatively soft Cu-Al coatings in particular have been evaluated by several researchers for their fretting fatigue properties [26,27]. Although APS was the dominant deposition technique to spray Cu-Al coatings, several case studies on flame spraying, laser cladding, electric spark, and cathodic arc were also conducted by researchers as other means of deposition [28–30]. However, to the authors' best knowledge, HVOF has not previously been used to spray Cu-Al powder to investigate their tribological properties. Thus, the main purpose of this study is to critically evaluate the tribological behavior of Cu-10Al coatings deposited by means of HVOF and APS. The coating microstructure was characterized, and microhardness was measured. The wear performance of the Cu-10Al coatings was tested at room temperature (RT), 300°C, and 450°C and correlated to the interfacial processes identified through ex-situ analysis. The current research on the Cu-10Al coatings sheds light on the influence of HVOF on the tribological performance of the coatings and investigates the complexity associated with their microstructural evolution during wear testing at room- and higher- temperatures.

4.3 Experimental Methods

4.3.1 Materials and coating preparation

Commercially available, mechanically clad, Cu-10Al (Metco 445, Oerlikon Metco, USA) with a particle size range of - 106 + 45 μm were used as feedstock powders in this study. These powders are high purity powders (~99%). Low carbon steel with dimensions 1"×1"×0.17" (25.4mm × 25.4mm × 4.3mm) were used as substrate materials. The steel substrate surfaces were grit-blasted using 80-grit alumina abrasive particles to increase the surface roughness and improve adherence of the coatings to the substrates. Cu-Al coatings were deposited on the grit-blasted substrates via HVOF (Oerlikon-Metco Diamond JetTM 2700 Gun, USA) and APS (radial injection 3-MB plasma gun, Oerlikon Metco, USA). The deposition parameters are tabulated in Table 4.1

for HVOF and in Table 4.2 for APS. The particle in-flight temperature and velocity were monitored using Accuraspray (Tecnar, Quebec, Canada) for both processes.

Table 4. 1 HVOF parameters

Parameter	Values
Gun transverse speed (m/s)	1
Number of passes	50
Feed rate (g/min)	30
Propylene flow rate (L/min)	77
Oxygen flow rate (L/min)	127
Air flow rate (L/min)	463
Spraying distance (mm)	225
Substrate mean temperature (°C)	145
In-flight particles temperature (°C)	2155
In-flight particles velocity (m/s)	227

Table 4. 2 APS parameters

Parameter	Values
Gun transverse speed (m/s)	1
Current (A)	500
Power (kW)	30
Number of passes	20
Powder feed rate (g/min)	32
Primary gas (Ar) flow rate (L/min)	6
Secondary (H) gas flow rate (L/min)	46
Spraying distance (mm)	64
Substrate mean temperature (°C)	565
In-flight particles temperature (°C)	2414
In-flight particles velocity (m/s)	204

4.3.2 Wear tests

Wear tests were performed on the as-sprayed coatings using a ball-on-flat reciprocating tribometer (Anton Paar TriTec SA, Switzerland). Prior to testing, the surface roughness was analyzed using a confocal laser microscope (Olympus LEXT 4000, USA), which was approximately 22 ± 2 µm for both coatings. A 6.35 mm alumina (Al2O3) ball was used as a counter body against the unpolished Cu-Al coatings. This was performed to understand the performance

of the coating without any surface finishing processes, which would help reduce the lead time and overall component cost. Further, Al_2O_3 was chosen as a counter body due to its high hardness and high thermal stability at elevated temperatures. Table 4.3 shows the parameters of the wear test. The testing was employed at three temperature conditions, room temperature (RT), 300°C and 450°C. Scanning Electron Microscope (SEM) and Energy Dispersive Spectroscopy (EDS) were employed to determine the wear surface morphologies and identify the eventual formation of tribolayers at the surface and cross-section of the wear tracks. The counter body surfaces were also analyzed after the testing to determine the eventual formation of a transfer film. To determine the statistical significance of the observed differences in wear rate between the HVOF and APS coatings at RT and 450 °C, a Hypothesis test was performed with a confidence level of 80%. The test was chosen based on the nature of the data and assumptions made about the distribution of wear rate values. The null hypothesis was that the wear rate of the HVOF coating is higher than APS coating, and the alternative hypothesis was that wear rate of the HVOF coating is lower than or equal to APS coating. The results of the statistical analysis were used to draw conclusions about the effectiveness of the temperature on reducing wear rate.

Table 4. 3 Ball-on-flat reciprocating wear test parameters

Parameter	Values
Applied load (N)	5
Frequency (Hz)	1
Stroke length (mm)	10
Sliding velocity (cm/s)	3.14
Number of cycles	5000
Total sliding distance (m)	100
Counter ball diameter (mm)	6.35 (Alumina ball)

4.3.3 Microstructural characterization

The microstructure and chemical composition of the as-sprayed coatings, as well as the wear tracks, were characterized by a field emission scanning electron microscope (FE-SEM) (SU8230, Hitachi, Japan) built with energy dispersive spectroscopy (EDS). Cross-sections were prepared as per the standard on metallographic preparation (ASTM E03). The coating thicknesses were evaluated from the obtained cross-section images. The average coating thickness was

determined, and standard mean error was reported. X-Ray Diffraction analysis (XRD) (X'pert, Malvern Panalytical, UK) was performed using a copper source (Cu Kα radiation (λ = 1.5406 Å)) with a scan rate of 2 deg/min. Microhardness tests using a Vickers microhardness tester (Anton Paar Micro Combi Tester, MCT3, Switzerland) were performed at RT, and target temperatures of 300°C and 450°C on polished coating surfaces. The actual high temperatures were 235°C and 345°C. Microhardness tests were also performed on a sample that had been exposed to 450°C, then cooled to RT: this is expected to have oxidized the sample (RT-oxidized). A 1000 mN load with a dwell period of 10 seconds was employed to generate at least 10 indentations (n = 10) on both coatings. The average microhardness value with its standard deviation was reported in each case.

4.4 Results

4.4.1 Microstructure, characterization, and microhardness

The cross-sections of both Cu-Al coatings are presented in Fig. 4.1. The SEM elemental maps of the cross sections are also presented in Fig. 4.1. The thickness of both coatings was measured to be 275 ± 25 μm, and the deposition efficiency of HVOF and APS spraying processes were 26% and 69%, respectively. The HVOF Cu-Al coating cross-section (Fig. 4.1a) exhibits a dense splat-on-splat structure formed by semi-flattened copper particles (light regions) covered by aluminum elements (dark areas) with a relatively low porosity. The APS coating (Fig. 4.1b) has a more homogenous microstructure comprised of light (copper), gray (aluminum), and dark gray (porosity) areas. These are in line with the EDS mapping (shown in Fig. 4.1), which also shows the presence of copper, aluminum, and low oxygen content. Notably, the distribution of oxygen is more prevalent in the Al phase in both coatings. The surface roughness of both as-deposited coatings was also similar (Sa = 20 ± 2 μm). Also, larger amount of aluminum – dark areas in the SEM cross-section of Fig. 4.1a – can be seen between HVOF coating splats than APS that depicts the lower temperature process. As is observed from Tables 4.1 and 4.2, particle velocities are relatively higher and particle temperatures are lower in HVOF (227 m/s and 2155°C) compared to APS (204 m/s and 2414°C).

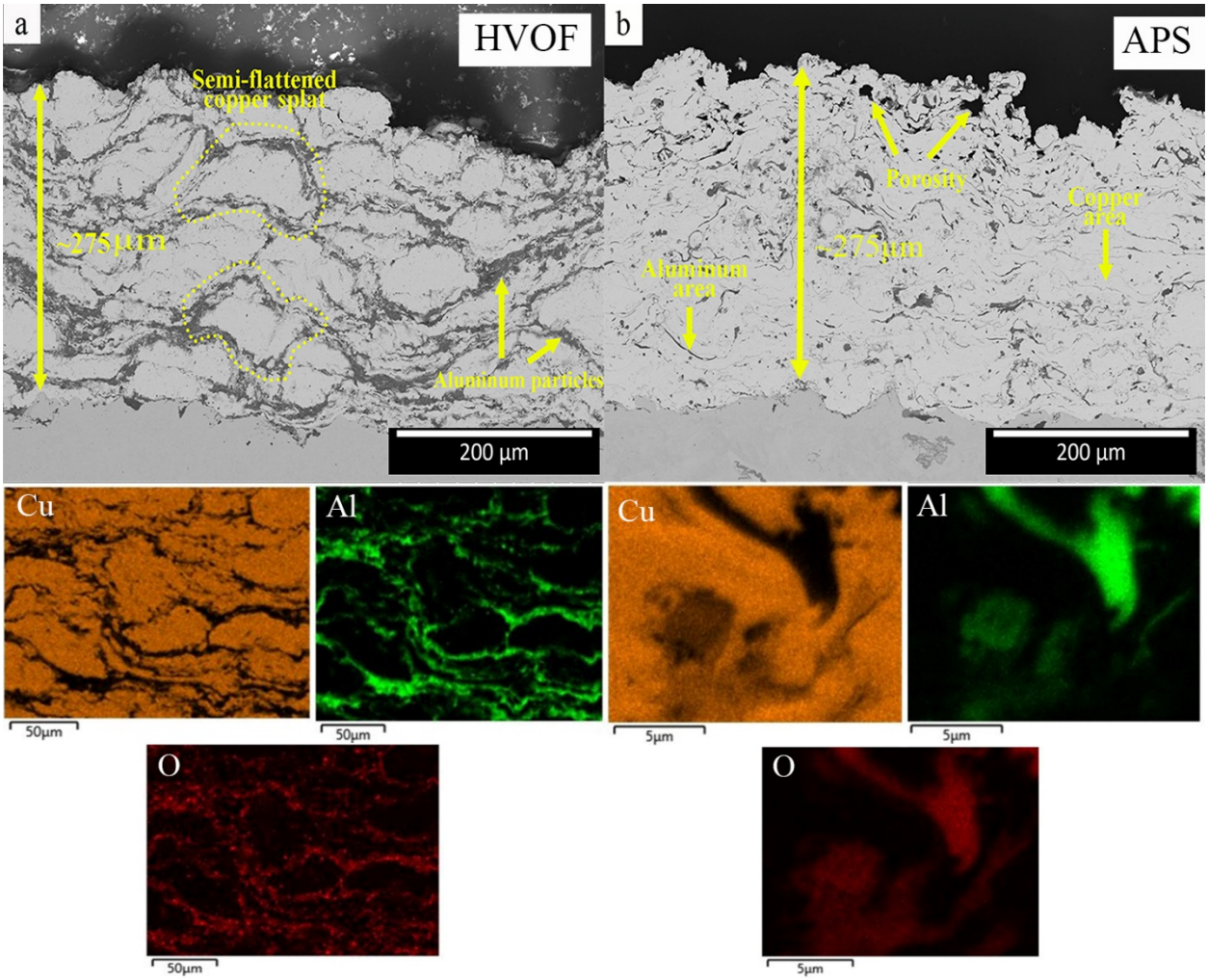

Figure 4. 1 Cross-sectional SEM images and elemental map analysis of the Cu-10Al coatings produced by (a) HVOF and (b) APS

The XRD patterns of the as-sprayed HVOF and APS coatings are presented in Fig. 4.2a and 4.2b. In both coatings, diffraction peaks of Cu, Al, and Cu_2O appeared while a peak of the intermetallic Cu_9Al_4 was detected for the HVOF coating. This can be interpreted by the fact that HVOF leads to less oxidation compared to APS, due to operating at lower temperatures as can be seen from the particle and substrate temperatures of Table 4.1 and Table 4.2. The higher Al content in the HVOF would likely be due to its larger presence in the coating in its natural state (Fig. 4.1a) whereas in the APS coating, the Al could be dissolved it the Cu matrix (solid solution, up to 18% Al in Cu) due to the high plasma temperatures.

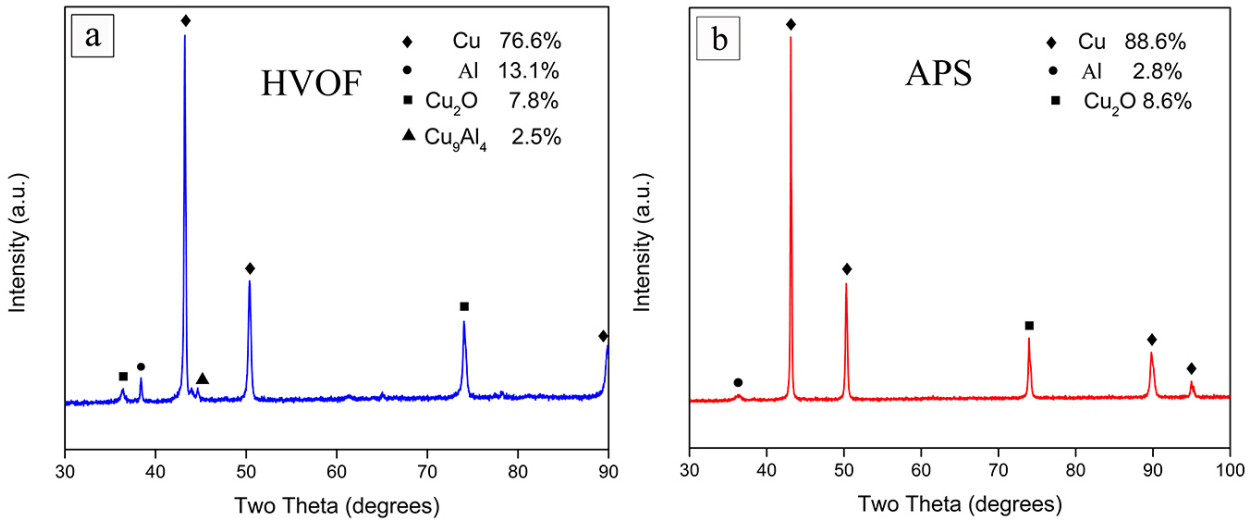

Figure 4. 2 XRD patterns of Cu-10Al coatings deposited by (a) HVOF and (b) APS

The average microhardness values are shown in Fig. 4.3. It can be observed that the microhardness of both coatings decreased as the temperature increased and that the APS coating has lower microhardness values than the HVOF coating. The HVOF RT-oxidized sample shows a notable increase of the coating microhardness as compared to the RT measurement, while no difference can be observed between the APS RT and RT-oxidized coatings.

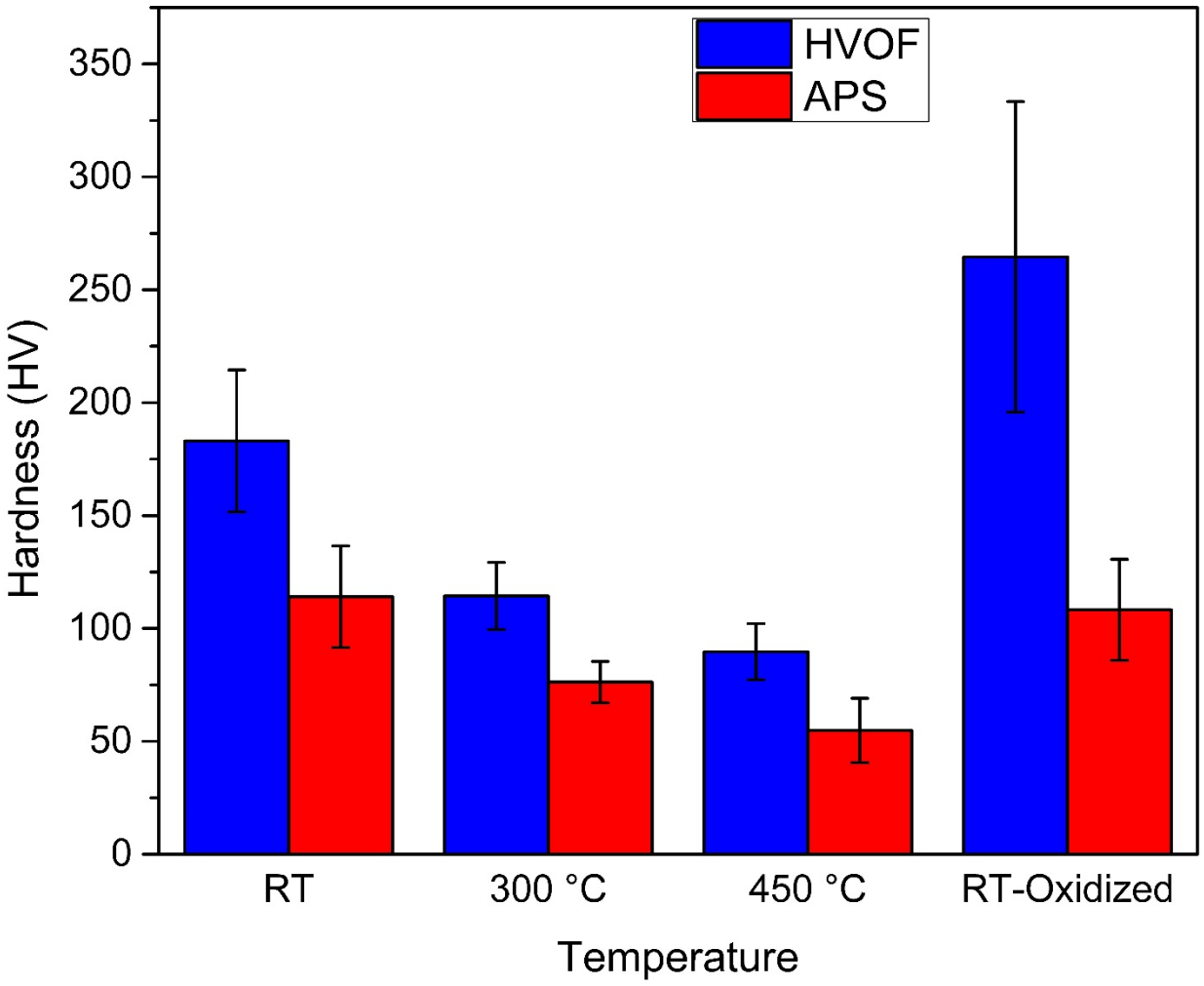

Figure 4. 3 Vickers microhardness of HVOF and APS developed Cu-10Al coatings at different temperatures

4.4.2 Friction coefficients and wear behaviors

The coefficient of friction as a function of the sliding cycles and test temperature is presented in Fig. 4.4. Both coatings illustrate similar behavior at RT, with a slight increase in the initial 1000 sliding cycles (running-in regime), following a constant steady state trend around 0.75 until the end of the test. At 300°C, the coefficient of friction of the HVOF increased from 0.2 to 0.73 at around 400 cycles and stabilized gradually around 0.7 up to the end of the test. On the other hand, this value for the APS coating decreased sharply from a peak of 0.75 to 0.5 at around 500 cycles, fluctuating around 0.6 for the rest of the test. At 450°C, after a short number of cycles (250

cycles), both coatings display the same variations at around 0.6 and 0.5 for HVOF and APS coatings respectively.

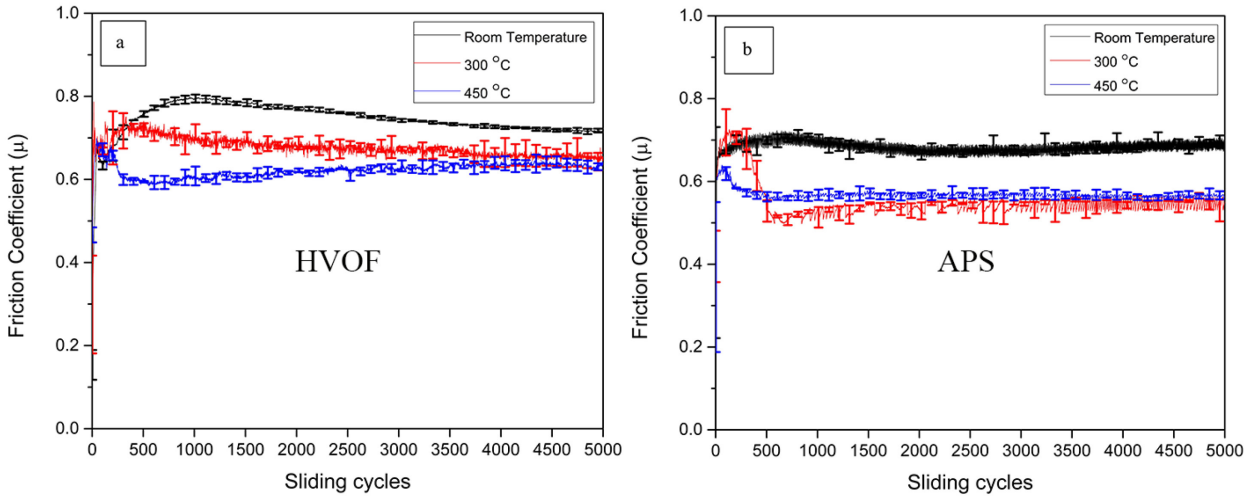

Figure 4. 4 Coefficient of friction of Cu-10Al coatings deposited by (a) HVOF and (b) APS at different temperatures

Figure 4.5 presents the specific wear rates of the coatings. It can be observed that both coatings have relatively low wear rate at RT, whereas at 300°C, the wear rate increases drastically. For the HVOF coating, the wear rate was 144.6 × 10^{-4} mm^3/N.m, which is 20% more than that of APS (114.2 × 10^{-4} mm^3/N.m) at 300 °C. At 450°C, the specific wear rate for both coatings decreased to less than half of their value at 300°C.. The statistical analysis was performed using a significance level of 20% (0.2). The results of the analysis indicated that the null hypothesis could not be rejected at this level of significance (as the P-value (0.157 for RT and 0.160 for 450 °C) was lower than 0.2), and therefore it was concluded that there is a difference in wear rate between the APS and HVOF coatings at RT and 450 °C. The finding suggests that the wear rate of the HVOF coating is higher than that of the APS coating, contrary to the alternative hypothesis. The observed difference in wear rate is statistically significant at the 20% significance level.

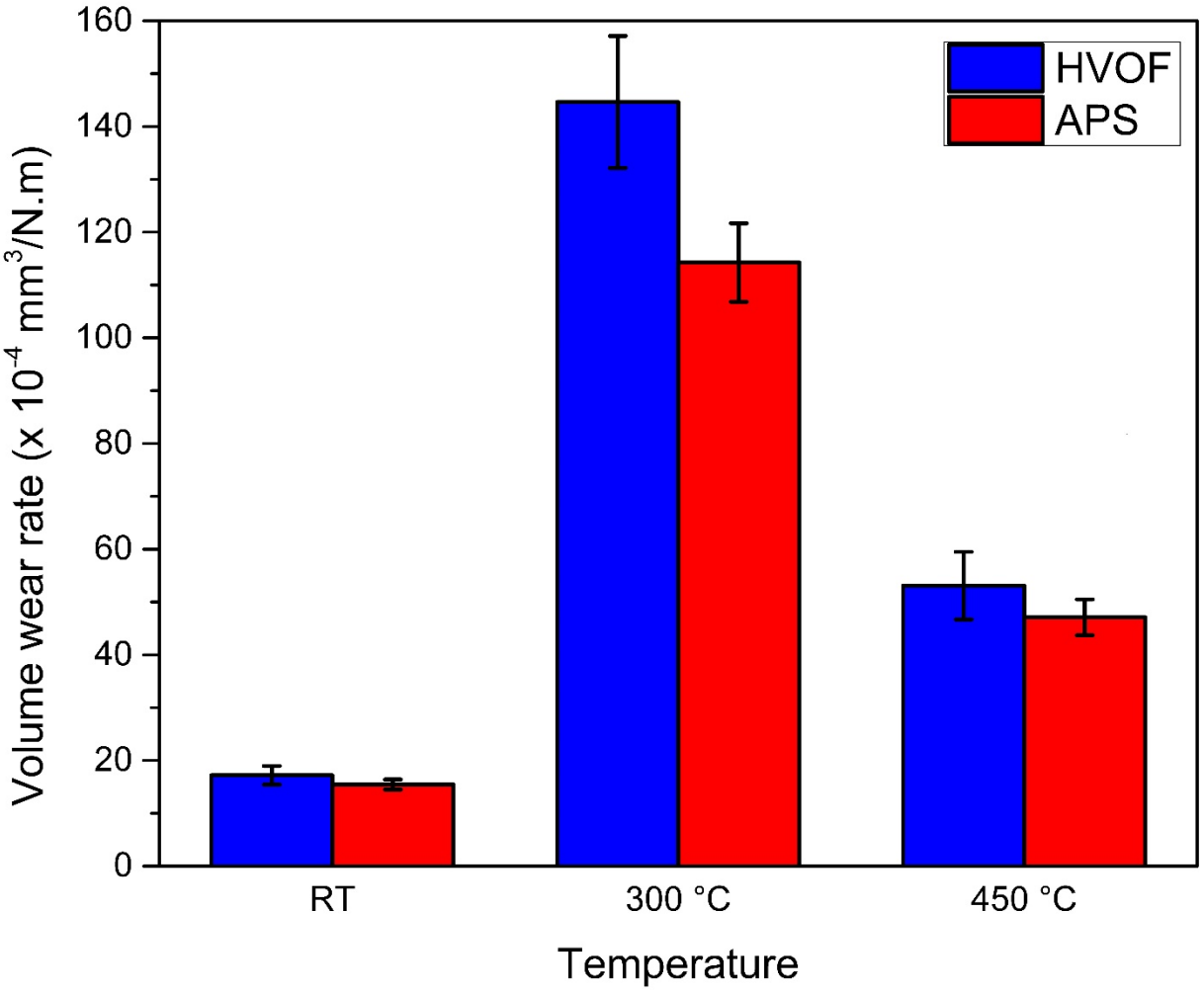

Figure 4. 5 Specific wear rate of Cu-10Al coatings produced by the HVOF and APS at different temperatures

Figure 4.6 shows the SEM images of the worn coating surfaces at RT, while the worn HVOF surface is comprised of delaminated layers with cracks (Fig. 4.6a), the worn APS surface has a more homogenous texture with smaller cracks and dispersed wear debris (Fig. 4.6b). It was confirmed from EDS color mapping (also in Fig. 4.6) that the worn surface of both coatings is rich in copper. EDS mapping on these worn surfaces also seemed to indicate that the worn APS coating (Fig. 4.6b) had higher oxygen content, possibly in the form of alumina, than the HVOF coating (Fig. 4.6a).

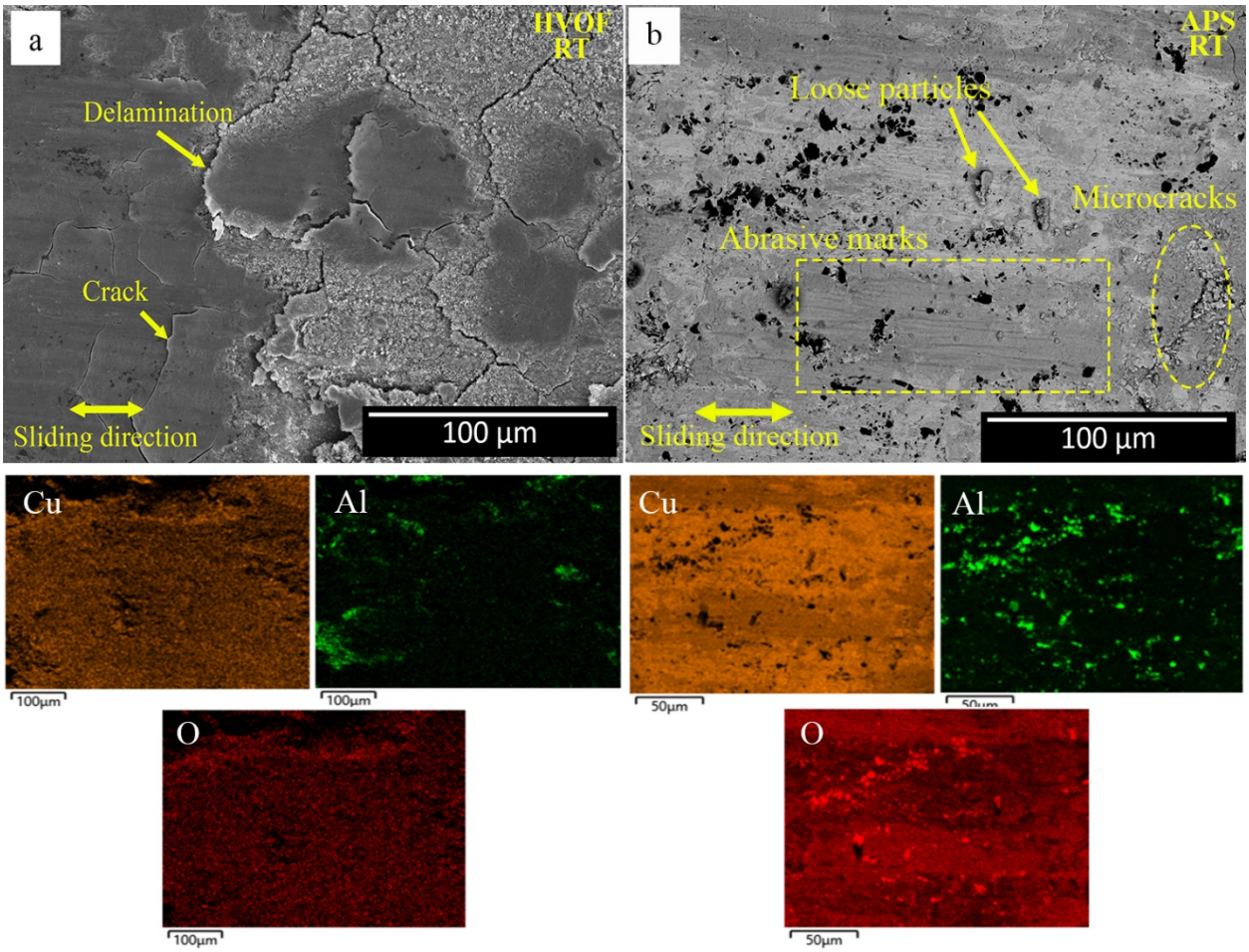

Figure 4. 6 SEM worn surface morphologies and elemental map analysis of (a) HVOF and (b) APS developed Cu-10Al coatings at RT

SEM images of the worn surfaces tested at 300°C are presented in Fig. 4.7. In HVOF, the presence of abrasive grooves and loose debris particles appeared throughout the worn surface (Fig. 4.7a) whereas the worn APS coating surface was mostly covered by potentially embedded debris particles with numerous cracks (Fig. 4.7b). It was observed that the width of the wear tracks at 300°C were quite higher than at RT and 450°C. EDS color maps are also presented in Fig. 4.7. These results notably showed a homogenous distribution of elements on the worn surface of both coatings at this temperature.

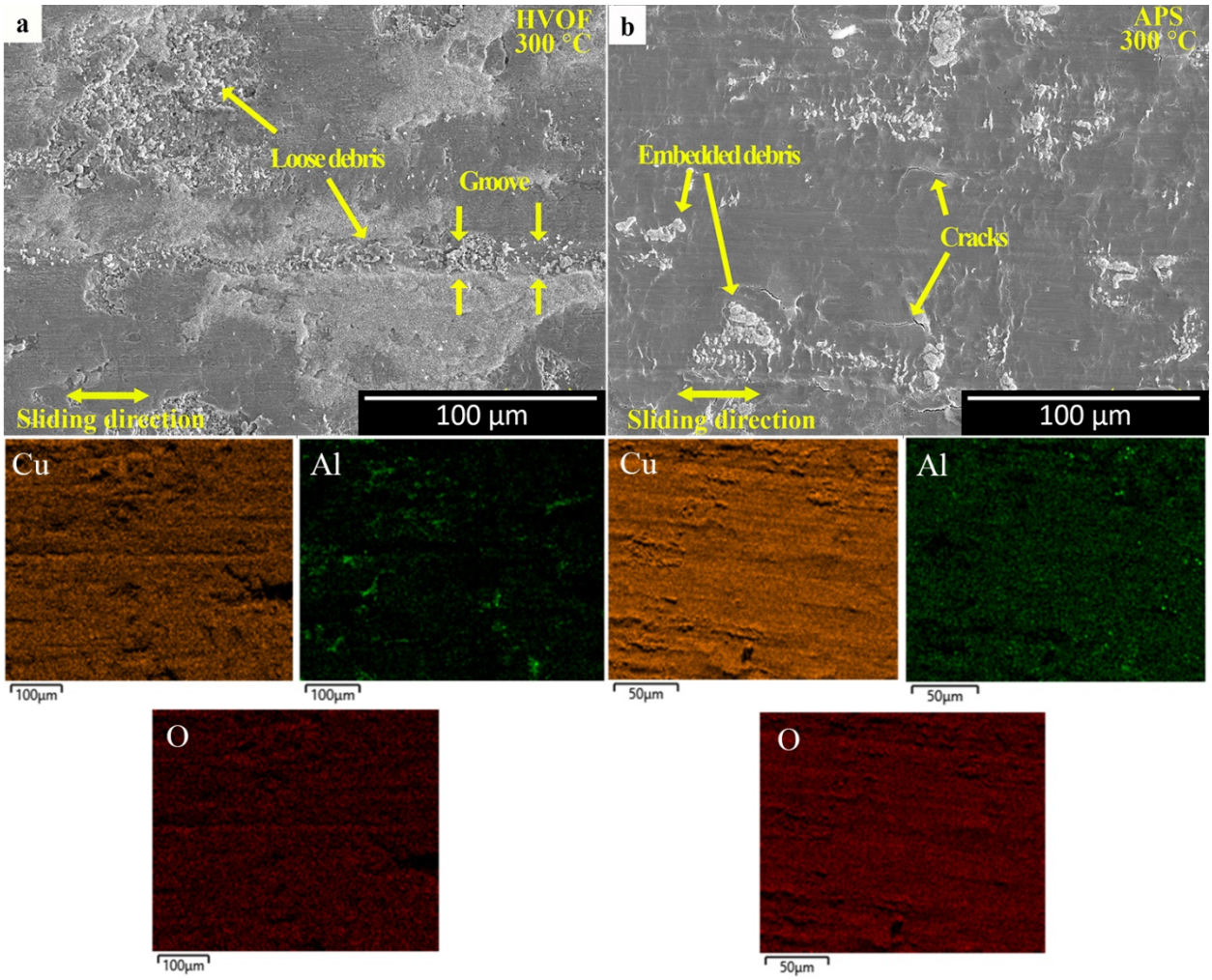

Figure 4. 7 SEM worn surface morphologies and elemental map analysis of (a) HVOF and (b) APS developed Cu-10Al coatings at 300 °C

Figure 4.8 displays the SEM images of the worn surfaces at 450°C. The SEM micrographs indicate a smeared layer on the worn surface of both coatings with seemingly less and smaller cracks. Moreover, EDS characterization was also conducted for the worn sliding surfaces at 450°C (also in Fig. 4.8) and the EDS mapping images depicted the highest amount of oxygen on the worn coating surface at this temperature. As is observed, higher concentrations of aluminum can be seen from the worn surface of the APS coating than HVOF coating.

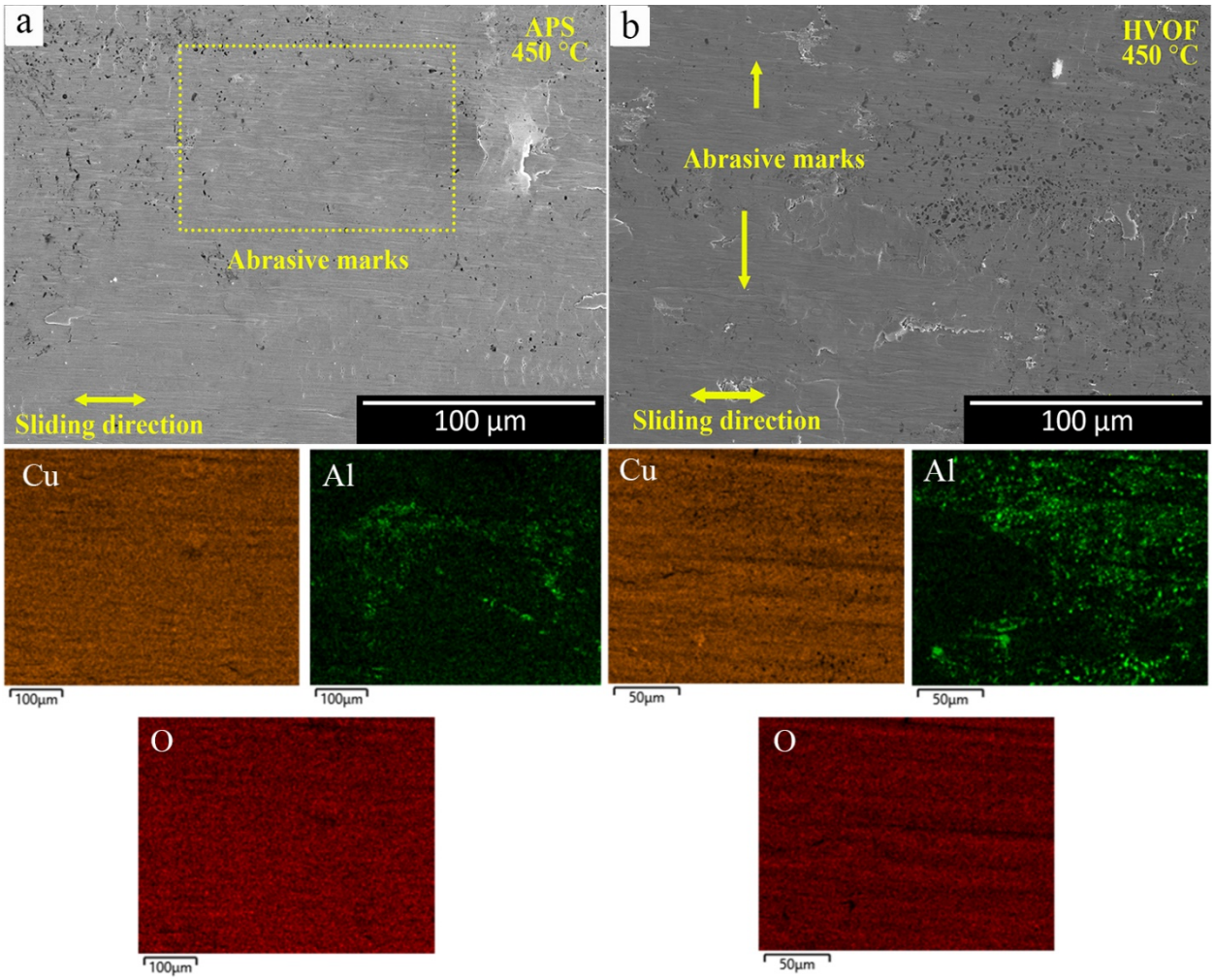

Figure 4. 8 SEM worn surface morphologies and elemental map analysis of (a) HVOF and (b) APS developed Cu-10Al coatings at 450 °C

Figure 4.9 shows cross-sectional micrographs of the worn HVOF and APS coatings subsurface at RT, 300°C, and 450°C. Thin tribo-films 3 ± 1 µm thick were formed on the surface of the APS and HVOF coatings at RT (Fig. 4.9a, 4.9b). Thicker mechanically mixed layer containing cracks (10 ± 4 µm) can be observed for both coatings at 300°C, as can be seen in Fig. 4.9c and 4.9d. Finally, 5 ± 2 µm thick tribo-films can be seen for the HVOF and APS coated samples tested at 450°C (Fig. 4.9e, 4.9f).

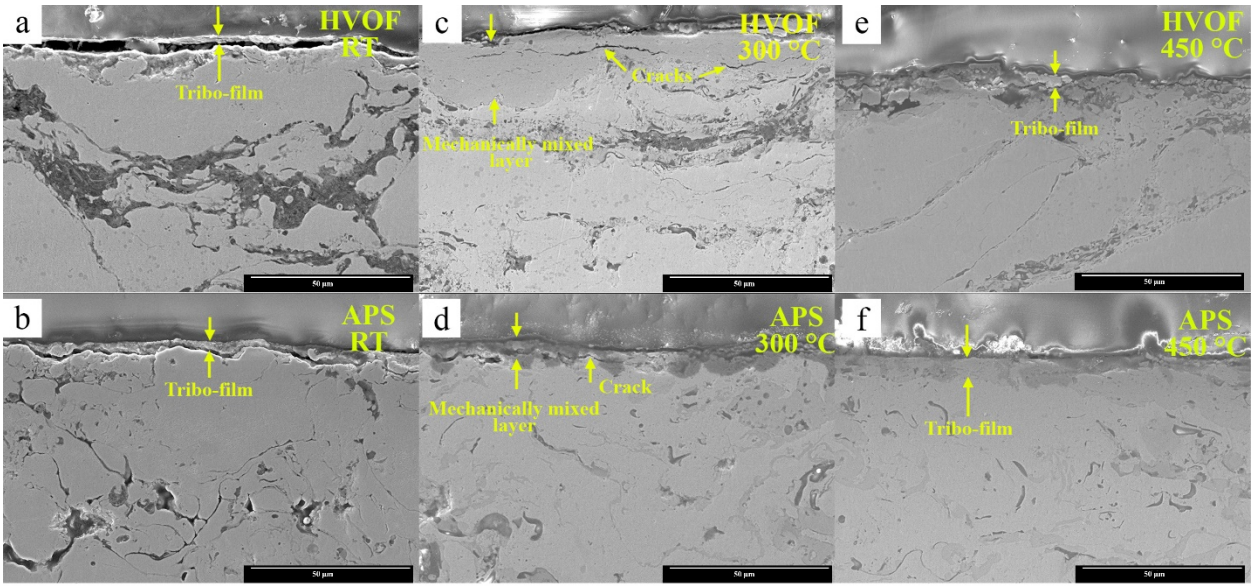

Figure 4. 9 SEM wear track cross-sections of HVOF and APS developed Cu-10Al coatings (a and b) at RT, (c and d) at 300 °C, and (e and f) at 450 °C

Figure 4.10 shows the EDS color maps of the worn HVOF and APS coatings cross sections at RT, 300°C, and 450°C. In line with the elemental mapping of the worn surfaces at different testing temperatures, the highest oxygen content can be observed from the formed tribo-film on both worn surfaces at 450°C (Fig. 4.10e and 4.10f). Oxygen-rich regions are also observed from the mechanically mixed layers formed on the top area of the HVOF and APS coatings worn cross sections (Fig. 4.10c and 4.10d) at 300°C, whereas tribo-films formed at RT seem to indicate the least accumulation of oxygen (Fig. 4.10a and 4.10b).

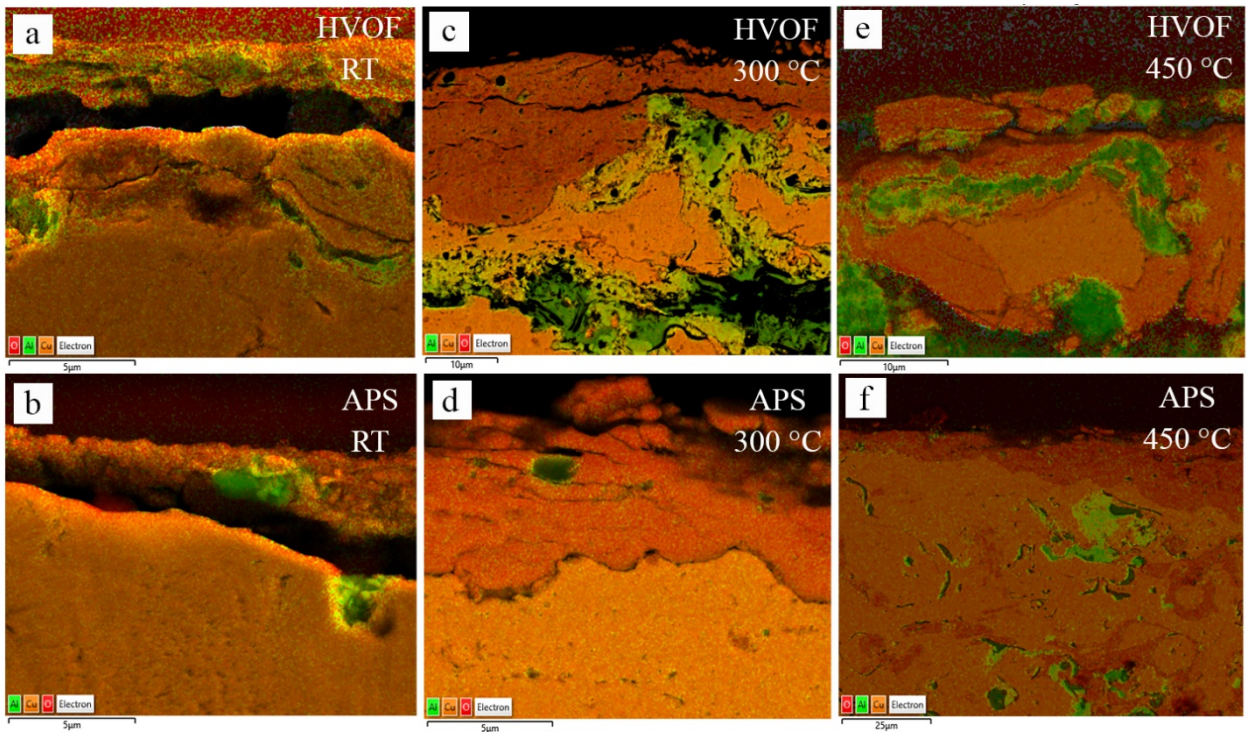

Figure 4. 10 Elemental map analysis of the wear track cross-sections of HVOF and APS developed Cu-10Al coatings (a and b) at RT, (c and d) at 300 °C, and (e and f) at 450 °C

The SEM micrographs of the alumina counter-balls after sliding against the coatings at RT and higher temperatures are presented in Fig. 4.11. Although slight layer transfer occurred on the counterparts at RT (Fig. 4.11a and 4.11b), relatively more transfer of materials to the alumina counterparts was observed at 300°C (Fig. 4.11c and 4.11d). Fig. 4.11e and 4.11f illustrate a milder transfer layer on the sliding counter parts slide at 450°C, as compared to the other conditions.

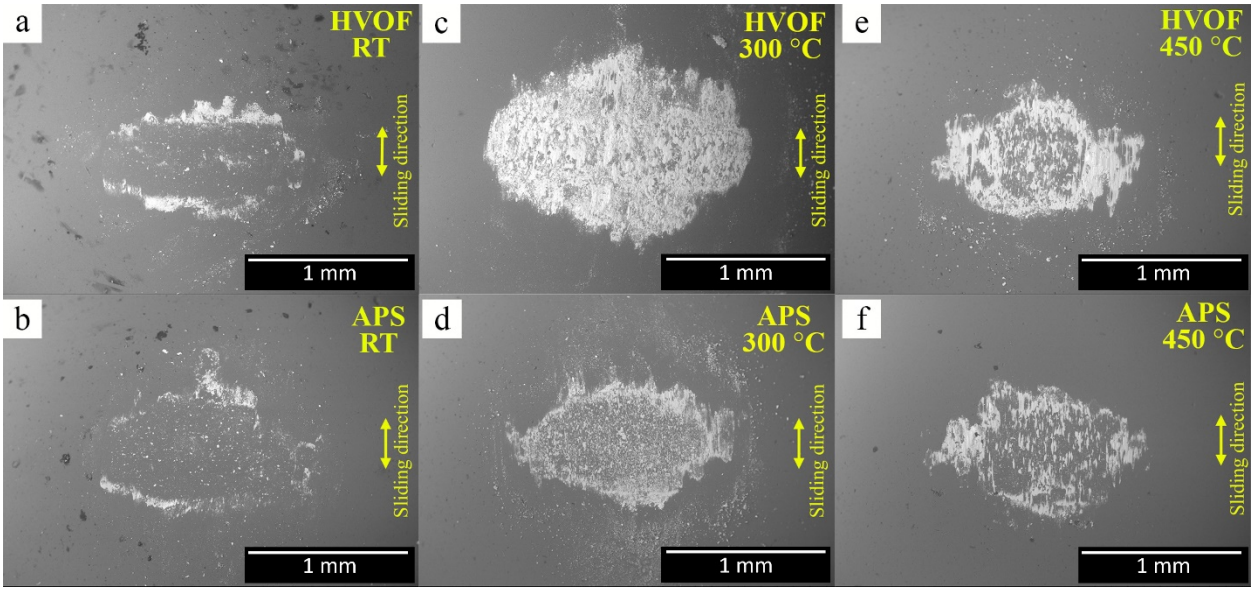

Figure 4. 11 SEM images of the alumina counter-balls sliding against Cu-10Al coatings at different temperatures: (a and b) HVOF and APS at RT, (c and d) HVOF and APS at 300°C and (e and f) HVOF and APS at 450°C

4.5 Discussion

4.5.1 Microstructure, characterization, and microhardness

Based on the microstructures shown in Fig. 4.1, it appears that the HVOF sprayed Cu-10Al particles were mostly plastically deformed, as they retained most of their initial morphology when observed in the cross-section (Fig. 4.1a). Thus, it can be inferred that particles remained un-molten or semi-molten during the HVOF process. On the other hand, the cross-section of the APS coating (Fig. 4.1) shows a lamellar structure, with little visible aluminum from the initial clad feedstock, implying that the coating was built by the accumulation of molten particles impacting on the substrate surface. As a result, this could lead to increased oxidation of the deposited metal powder during spraying for the APS coating [27]. In a similar study, Rakhunde et al. concluded that the APS Ni-based coating retains more oxides and higher porosity than the HVOF coating due to low particle velocity and higher particle temperature during the process [31]. This finding is aligned with the results shown in Table 4.1 and Table 4.2, exhibiting lower particle velocity and higher particle temperature for the APS spray conditions as compared to the HVOF spray conditions. The XRD analysis is also consistent with this idea as it shows higher oxide contents in the APS coating compared to the HVOF coating. These results are in agreement with the results from EDS

characterization (Fig. 4.1), which indicate a greater amount of oxide between APS splats compared to HVOF ones (shown in Fig. 4.1).

The results obtained from the Vickers microhardness measurements (Fig. 4.3) indicate that the HVOF-sprayed coatings are harder than the corresponding APS coatings. Increased microhardness of the coating is a major characteristic of the HVOF method. The high particle velocity in this process rendered high plastic deformation of the splats/particles and therefore exceptional hardness would be achieved [32]. Similar observation has been reported by Gassot et al. [33] on the microhardness of copper coatings sprayed by HVOF and APS techniques. In addition, a low amount of porosity, with no interconnected pores, is observed from bottom to top regions of the HVOF coating (Fig. 4.1a) while higher amount of porosity can be seen, particularly close to the top regions, in the APS coating with a homogenous dispersion of oxide throughout the coating (Fig. 4.1b). Since porous microstructure have lower hardness, the APS coating, with a larger amount of pores, would have lower microhardness than the HVOF coating [34], as observed here (Fig. 3). This is further supported by Bolelli et al. who found lower microhardness values for Al_2O_3 and Cr_2O_3 oxides in all temperatures for porous APS coating as compared to dense HVOF coating, under a 1000 mN indentation load [35]. The authors associated the lower hardness of the APS coating with extensive interlamellar failure, and the higher hardness of the HVOF coatings with less oxide content that bore less damage during indentation test. Kamal et al. also performed a comprehensive experiment on the correlation of porosity and hardness in aluminum-based coating produced by micro-arc oxidation process. They found out that the porosity and hardness in the resulted coating are inversely proportional [36].

As for the general evolution of the hardness with increasing temperature (Fig. 4.3), it was observed that the feedstock in the HVOF process was not fully melted and underwent a high-degree of plastic deformation. Consequently, this would lead to work-hardening of the feedstock and an increase in the strain and defects (dislocations, etc.) within the coating [37]. Thus, with increasing temperature, softening of the work-hardened metallic material may have caused a noticeable reduction of the microhardness for the HVOF coating (Fig. 4.3). On the other hand, for the APS coating, while the coating might be oxidized, there is still the characteristics of a metallic structure with defects such as dislocations. As a result, softening of the metal matrix would lead to the decrease in the microhardness of the coating material. Interestingly, a marked increase in the

microhardness value of the HVOF coating after microhardness testing at RT (i.e. after -exposure to 450°C for 90 mins) (Fig. 4.3) was observed. At the same time, the APS hardness remained nearly unchanged. This could be attributed to the oxidation of the HVOF coating at 450°C, highlighting the idea that the as-sprayed HVOF coating shows relatively low oxidation. In contrast, the lack of change in hardness for the APS coating would be associated with the already highly oxidized as-sprayed conditions.

4.5.2 Friction and wear behavior

The wear rates for HVOF coating at RT is higher (Fig. 4.5), despite the HVOF coating possessing higher hardness values (Fig. 4.3). Even though the hardness of the material is generally recognized as the critical factor for its abrasive wear resistance in this work, the harder HVOF coatings, possessed higher wear rate than the APS coatings. This shows a non-linear dependence of wear rate on hardness of the abraded coating. The higher wear rates of the HVOF coating at RT when compared to the APS coating might be due to the brittle fracture of the top layers of the coating (Fig. 4.6a). This can be seen from continuous cracks and delamination on the worn surface of this coating. The APS coating, however, was mostly covered by wear debris particles with fewer microcracks (Fig 4.6b). Bolelli et al. [39] proposed interlamellar failure as the preferential crack propagation path for the worn surface of Al_2O_3 and Cr_2O_3 oxide coatings deposited by APS, and this could be related to the melted particles during the deposition process. This, in turn, could have reduced the possibility of crack formation as is obvious from the smoother surface of APS coating with no evidence of delamination. Also, this decrease in the wear volume of APS coating could be related to more alumina content on the worn surface of this coating as hard alumina particles tend to contribute significantly to the wear resistance (Fig. 4.6). It should be noted that the alumina particles are less likely to have originated from the counterface since there has been no wear identified from the alumina ball. Additionally, the formation of a smooth and continuous tribo-film on the worn surface of both coatings at RT might have performed as a protective layer during sliding, as observed in Fig. 4.9a and 4.9b when compared to the coatings performed at 300 °C. Liu et al. also reported the formation of Cu_2O in the form of thin oxygen-rich areas at the sample surface after several sliding cycles at RT [40]. Furthermore, the counter-balls would mostly slide on the formed tribo-film of the tested coatings, causing the lowest observed wear rate for both coatings at RT. This can also be observed from the SEM images of the alumina counter-balls (Fig.

4.11a and 4.11b) with little transfer film from both coatings to the contact zones. As a result, abrasive wear would appear as the dominant mechanism for both coatings during sliding at RT, and it would be relatively limited with these Cu-Al coatings.

At higher temperatures, significant wear rate differences emerge. When increasing the temperature to 300°C, the wear rate increased markedly for both coatings (Fig. 4.5), while the hardness of the coatings decreased (Fig. 4.3). Also, the material transfer to the alumina counter-balls against the worn surface of both coatings seems more prevalent as compared to the counter-faces slid at RT and 450°C (Fig. 4.11). This may be explained by the softening of the metallic copper at this temperature as well as by the formation of detrimental unstable and thick mechanically mixed layer [41], as was observed in Fig. 4.9c and 4.9d. In addition, from elemental distribution maps of the worn surface cross sections (Fig. 4.10c and 4.10d), it was confirmed that mechanically mixed regions are rich in oxygen. Quinn et. al. [43] reported that the formation of tribo-oxides cannot protect the surface from wearing off due to crack propagation when tribo-oxide layers reach a critical thickness, which could be associated with the poor wear resistance of the coatings obtained at 300°C (Fig. 4.5). More specifically, it appeared that the APS coating had better wear resistance than the HVOF coating (Fig. 4.5) at 300°C, although having a comparable hardness value (Fig. 4.3). The higher wear rate of the HVOF coating could be explained by more material transfer to the counter-ball sliding on the HVOF coating (Fig. 4.11c) than for the APS coating (Fig. 4.11d). The worn surface of the HVOF coating also shows more loose debris than the APS coating (Fig. 4.7), and these could also lead to the abrasive grooving of the surface (Fig. 4.7a). These wear debris notably indicate a different wear mechanism than the one observed at RT. It is possible that the difference in the distribution of aluminum within the coatings (Fig. 4.1a and 4.1b) would have led to different bonding reactivity with the alumina counter-balls at 300°C, and notably led to a higher amount of transfer to the HVOF coating than the APS coating. In turn, this could have caused a different behavior in the generation of debris particle and led to a higher wear rate for the HVOF coating than the APS coating. This difference can also be confirmed by the higher friction value for the HVOF coating at 300°C as observed in Fig. 4.4. It is known that the coefficient of friction can be divided into two components:

$$\mu = \mu_d + \mu_b \quad (1)$$

Where μ_d is the adhesive component and μ_b is the abrasion term [44]. Therefore, it would appear that wear was dominated by abrasion in the APS coating at 300°C, while there was an additional contribution to adhesion in the HVOF coating, which is supported by the higher amounts of material transfer to the counter-ball, as well as the increased friction.

At 450°C, however, the wear rate decreased significantly (Fig. 4.5) while the hardness continued reducing for both coatings (Fig. 4.3). Considering the actual temperature during the test (330°C for a 450°C target temperature), the temperature is 50% of the melting point of aluminum and 30% of the melting point of copper. Lenard et al. found that partial or complete softening of the microstructure takes place by static recrystallization in which the operating mechanisms are density reduction and the change in the dislocation distribution after being exposed to high temperature [45]. Therefore, static recrystallization would be a possible mechanism to dissipate and decrease dislocations and increase the grain size. This, in turn, may trigger a decrease in hardness with an increased cohesion and a more ductile behavior of both coatings, at this higher temperature (450°C) (Fig. 4.5). However, the lower wear rate of the APS coating can be explained by slightly higher amount of alumina dispersed on the worn surface of this coating which improved the wear resistance (see Fig. 4.8). It can also be due to the formation of a thin stable continuous tribo-film on the worn surface of both coatings (Fig 4.9e and 4.9f) which showed the highest content of oxygen among all the worn coatings (Fig. 4.10e and 4.10f). Stachowiak and Batchelor also pointed out the formation of smooth surfaces can be caused by localized plastic deformation due to large contact stresses between contacting materials [46]. A larger amount of softening at 450°C may have led to the reduction of the shear strength of the coating, ending with friction coefficient reduction in both coatings (Fig. 4.4) [41]. There is also indication of abrasive marks in the SEM images of the worn surfaces at this temperature (Fig. 4.8a and 4.8b). Like for the 300°C counter-balls, adhesive films transferred at the contact surfaces (Fig. 4.11e and 4.11f). However, the transfer film was found to be covering smaller area fraction at the contact zone at 450°C. Therefore, although adhesive and abrasive wear mechanisms were active at 450°C, the abrasion wear mechanism with the formation of tribo-film seems to predominantly control the wear performance of both coatings.

4.5.3 Proposed wear mechanism

The wear mechanisms under different conditions can be described by schematic diagrams, as shown in Fig. 12. At RT, although the presence of cracks with material delamination for HVOF and microcracks and loose debris for APS results in wear volume loss with greatest value of friction coefficient in this study, the lowest wear rate for both coatings was governed by the formed continuous tribo-film (Fig. 4.4, 4.5, 4.6a-b, and 4.9a-b). The wear mechanism was abrasive for both coatings at this temperature with the lowest amounts of transfer film adherence to the counter balls of the study (Fig. 4.11a-b). At 300°C, the wear mechanism is mainly the synergy of abrasive and adhesive wear with a higher friction coefficient for HVOF coating as compared to APS coating in which abrasive wear was prevalent with a lower friction coefficient (Fig. 4.4). Larger loose debris and long parallel grooves are produced on HVOF coating wear track which caused serious wear volume loss (Fig. 4.5 and 4.7a). Similarly, numerous cracks and embedded particles present on the wear track of APS coating were the rationale for high wear rate (Fig. 4.5 and 4.7b). Additionally, the formation of weak and unstable mechanically mixed layers containing cracks resulted in a significant transfer of mating materials to the alumina counter balls (Fig. 4.9c-d and 4.11c-d). At 450°C, although abrasion wear and abrasive wear are active, the main wear mechanism was abrasive due to the presence of parallel scratches on the wear track of both coatings (Fig. 4.8a-b). Relatively, lower wear rate and lower transfer film formation on the counter balls at this temperature can be attributed to the generation of a tribo-film on the wear track (Fig. 4.5, 4.9e-f, and 4.11e-f).

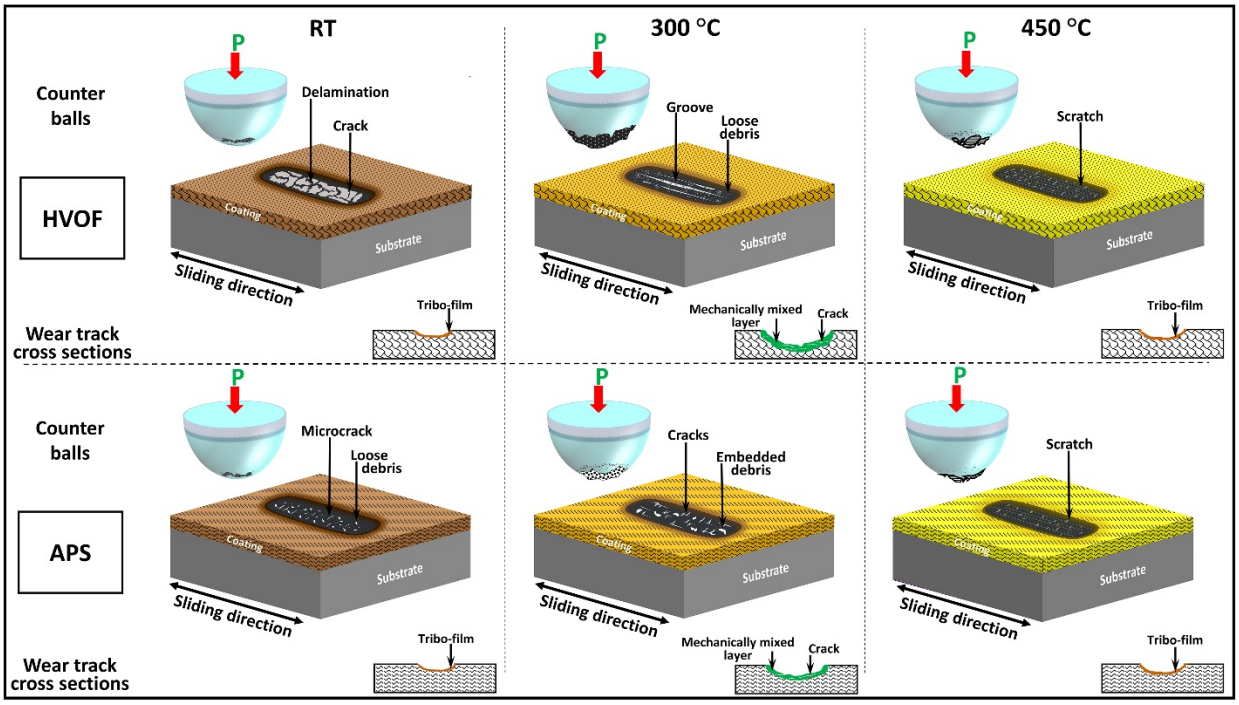

Figure 4. 12 Schematic of wear mechanisms of the Cu-Al HVOF and APS coatings at RT, 300 °C and 450 °C

4.6 Conclusion

In this study, the tribological performance of thermally sprayed Cu-10Al coatings sprayed by HVOF and APS was critically evaluated at room- and elevated- temperatures. In addition, the effect of the coating microstructure on the wear and friction behavior was discussed. More specifically, the cross-section micrographs of the HVOF coating showed an almost fully dense coating while the APS coating had a higher amount of porosity. The XRD analysis revealed that the formation of oxide in the HVOF coating was lower than the APS coatings. Vickers microhardness values of the HVOF coating were higher than the APS microhardness for all tested temperatures due to the dense microstructure of this coating. The coefficients of friction of both coatings were substantially higher at RT compared to higher temperatures, while specific wear rates were the lowest at RT. The coatings at RT showed evidence of brittle fracture and interlamellar failure for the HVOF and APS coatings, respectively, leading to suggest abrasive wear as the main mechanism. At 300°C, wear was dominated by abrasion in the APS coating at 300°C, while there was an additional contribution to adhesion in the HVOF coating. Finally, at

450°C, abrasive wear seemed to be the main wear mechanism. The formation of a thin tribo-film layer at RT and 450°C might have protected the coating from wear, whereas a thicker and more unstable tribo-layer mechanically mixed layer might have caused more wear rate for both coatings at 300°C.. Based on the findings in this study, several open questions remain to be addressed. Notably, the optimal particle size distribution of the feedstock powder as well as the optimization of the HVOF spraying parameters would deserve further consideration, to explore possibly better coating wear properties.

References:

1. Barshilia HC. Surface Modification Technologies for Aerospace and Engineering Applications: Current Trends, Challenges and Future Prospects. Trans Indian Natl Acad Eng. 2021 Jun;6(2):173–88.

2. Advanced tribological coating solutions for next generation mechanical systems in extreme environments. In.

3. Stoyanov P, Dawag L, Goberman DG, Shah D. Friction and Wear Characteristics of Single Crystal Ni-Based Superalloys at Elevated Temperatures. Tribol Lett. 2018 Mar;66(1):47.

4. Stoyanov P, Dawag L, Joost WJ, Goberman DG, Ivory S. Insights into the static friction behavior of Ni-based superalloys. Surface and Coatings Technology. 2018 Oct;352:634–41.

5. Ross E, Ignatov A, Stoyanov P. Tribological Characteristics of Manufactured Carbon Under Extreme Contact Conditions. Tribol Ind. 2021 Sep 15;43(3):465–9.

6. Stoyanov P, Boyne A, Ignatov A. Tribological characteristics of Co-based plasma sprayed coating in extreme conditions. Results in Surfaces and Interfaces. 2021 May;3:100007.

7. Harrington KM, Miller EC, Frye A, Stoyanov P. Tribological insights of Co- and Ni-based alloys in extreme conditions. Wear. 2021 Jul;477:203827.

8. Roy A, Munagala VNV, Patel P, Sharifi N, Alidokht SA, Makowiec M, et al. Friction and wear behavior of suspension plasma sprayed tantalum oxide coatings at elevated temperatures. Surface and Coatings Technology. 2023 Jan;452:129097.

9. de Castilho BCNM, Munagala VNV, Alidokht SA, Sharifi N, Bessette S, Makowiec ME, et al. Insights on Silver Migration Mechanisms and their Influence on the Wear Behavior of Thermally Sprayed Self-lubricating Coatings Up to 350 °C. Tribol Lett. 2022 Dec;70(4):120.

10. Patel P, Alidokht SA, Sharifi N, Roy A, Harrington K, Stoyanov P, et al. Microstructural and Tribological Behavior of Thermal Spray CrMnFeCoNi High Entropy Alloy Coatings. J Therm Spray Tech. 2022 Apr;31(4):1285–301.

11. Bakshi SR, Harimkar SP. Surface Engineering for Extreme Conditions. JOM. 2015 Jul;67(7):1526–7.

12. Xue YJ, Zhang YZ. Surface coatings in tribological and wearresistant applications. International Heat Treatment and Surface Engineering. 2009 Jun;3(1–2):17–25.

13. Yin S, Cizek J, Suo X, Li W, Liao H. Thermal Spray Technology. Advances in Materials Science and Engineering. 2019 Jan 9;2019:1–2.

14. Lince J. Coatings for Aerospace Applications. 2017 [cited 2022 Dec 21]; Available from: http://rgdoi.net/10.13140/RG.2.2.21638.16964

15. Handbook of Environmental Degradation of Materials [Internet]. Elsevier; 2018 [cited 2022 Dec 20]. Available from: https://linkinghub.elsevier.com/retrieve/pii/C20160020818

16. Gupta G, Tyagi RK, Rajput SK, Maan R, Jacob S, Verma S. Review on Thermal Spray Coating Methods and Property of Different Types of Metal-Based Coatings. In: Sharma BP, Rao GS, Gupta S, Gupta P, Prasad A, editors. Advances in Engineering Materials [Internet]. Singapore: Springer Singapore; 2021 [cited 2022 Dec 22]. p. 427–39. (Lecture Notes in Mechanical Engineering). Available from: https://link.springer.com/10.1007/978-981-33-6029-7_40

17. Viswanathan V, Katiyar NK, Goel G, Matthews A, Goel S. Role of thermal spray in combating climate change. emergent mater. 2021 Dec;4(6):1515–29.

18. Hardwicke CU, Lau YC. Advances in Thermal Spray Coatings for Gas Turbines and Energy Generation: A Review. J Therm Spray Tech. 2013 Jun;22(5):564–76.

19. Pawlowski L. The Science and Engineering of Thermal Spray Coatings [Internet]. 1st ed. Wiley; 2008 [cited 2022 Dec 21]. Available from: https://onlinelibrary.wiley.com/doi/book/10.1002/9780470754085

20. Lima RS, Marple BR. From APS to HVOF spraying of conventional and nanostructured titania feedstock powders: a study on the enhancement of the mechanical properties. Surface and Coatings Technology. 2006 Mar;200(11):3428–37.

21. Lee H, Mall S, Sanders JH, Sharma SK, Magaziner RS. Characterization of fretting wear behavior of Cu–Al coating on Ti–6Al–4V substrate. Tribology International. 2007 Aug;40(8):1301–10.

22. Stoyanov P, Harrington KM, Frye A. Insights into the Tribological Characteristic of Cu-Based Coatings Under Extreme Contact Conditions. JOM. 2020 Jun;72(6):2191–7.

23. Ren W, Mall S, Sanders JH, Sharma SK. Degradation of Cu-Al Coating on Ti-6AI-4V Substrate under Fretting Fatigue Conditions. Tribology Transactions. 2003 Jan;46(3):353–60.

24. Jin O, Mall S, Sanders JH, Sharma SK. Durability of Cu–Al coating on Ti–6Al–4V substrate under fretting fatigue. Surface and Coatings Technology. 2006 Oct;201(3–4):1704–10.

25. Fridrici V, Fouvry S, Kapsa P. Fretting wear behavior of a Cu–Ni–In plasma coating. Surface and Coatings Technology. 2003 Jan;163–164:429–34.

26. Jin O, Mall* S, Sanders JH, Sharma SK, Hager CH. Fretting Fatigue Behavior of Cu-Al-Coated Ti-6Al-4V. Tribology Transactions. 2007 Oct 23;50(4):497–506.

27. Ranjan A, Islam A, Pathak M, Khan MK, Keshri AK. Plasma sprayed copper coatings for improved surface and mechanical properties. Vacuum. 2019 Oct;168:108834.

28. Lifan S, Yuan G, Dejun K. Effect of MoS2 mass fraction on microstructure and tribological characteristics of laser cladded Cu–10Al coating. Surfaces and Interfaces. 2022 Feb;28:101599.

29. Ren W, Mall S, Sanders JH, Sharma SK. Evaluation of coatings on Ti–6Al–4V substrate under fretting fatigue. Surface and Coatings Technology. 2005 Mar;192(2–3):177–88.

30. Morales, Piamba, Olaya. Influence of Gas Pressure on the Mechanical and Tribological Properties of Cu-Al Coatings Deposited via Thermal Spray. Coatings. 2019 Nov 1;9(11):722.

31. Rukhande SW, Rathod WS, Bhosale D. High-temperature tribological investigation of APS and HVOF sprayed NiCrBSiFe coatings on SS 316L. Tribology - Materials, Surfaces & Interfaces. 2022 Apr 3;16(2):98–109.

32. Singh V, Singh I, Bansal A, Omer A, Singla AK, Rampal, et al. Cavitation erosion behavior of high velocity oxy fuel (HVOF) sprayed (VC + CuNi-Cr) based novel coatings on SS316 steel. Surface and Coatings Technology. 2022 Feb;432:128052.

33. Gassot H, Junquera T, Ji V, Jeandin M, Guipont V, Coddet C, et al. Comparative Study of Mechanical Properties and Residual Stress Distributions of Copper Coatings Obtained by Different Thermal Spray Processes. Surface Engineering. 2001 Aug;17(4):317–22.

34. Kuroda S, Clyne TW. The quenching stress in thermally sprayed coatings. Thin Solid Films. 1991 May;200(1):49–66.

35. Bolelli G, Lusvarghi L, Manfredini T, Mantini FP, Polini R, Turunen E, et al. Comparison between plasma- and HVOF-sprayed ceramic coatings. Part I: microstructure and mechanical properties. IJSURFSE. 2007;1(1):38.

36. Kamal Jayaraj R, Malarvizhi S, Balasubramanian V. Optimizing the micro-arc oxidation (MAO) parameters to attain coatings with minimum porosity and maximum hardness on the friction stir welded AA6061 aluminium alloy welds. Defence Technology. 2017 Apr;13(2):111–7.

37. Brandt OC. Mechanical properties of HVOF coatings. JTST. 1995 Jun;4(2):147–52.

38. Abrasive, Erosive and Cavitation Wear. In: Engineering Tribology [Internet]. Elsevier; 2014 [cited 2023 Feb 10]. p. 525–76. Available from: https://linkinghub.elsevier.com/retrieve/pii/B9780123970473000114

39. Bolelli G, Lusvarghi L, Manfredini T, Mantini FP, Turunen E, Varis T, et al. Comparison between plasma- and HVOF-sprayed ceramic coatings. Part II: tribological behaviour. IJSURFSE. 2007;1(1):62.

40. Liu Z, Patzig C, Selle S, Höche T, Gumbsch P, Greiner C. Stages in the tribologically-induced oxidation of high-purity copper. Scripta Materialia. 2018 Aug;153:114–7.

41. Lehmann JS, Schwaiger R, Rinke M, Greiner C. How Tribo-Oxidation Alters the Tribological Properties of Copper and Its Oxides. Adv Mater Interfaces. 2021 Jan;8(1):2001673.

42. Quinn TFJ. Review of oxidational wear. Tribology International. 1983 Oct;16(5):257–71.

43. Schiffmann KI, Hieke A. Analysis of microwear experiments on thin DLC coatings: friction, wear and plastic deformation. Wear. 2003 Mar;254(5–6):565–72.

44. Lenard JG, Pietrzyk M, Cser L. Microstructure Evolution and Mechanical Properties of the Final Product. In: Mathematical and Physical Simulation of the Properties of Hot Rolled Products [Internet]. Elsevier; 1999 [cited 2022 Dec 23]. p. 151–236. Available from: https://linkinghub.elsevier.com/retrieve/pii/B9780080427010500061

45. Fundamentals of Contact Between Solids. In: Engineering Tribology [Internet]. Elsevier; 2014 [cited 2023 Jan 24]. p. 475–524. Available from: https://linkinghub.elsevier.com/retrieve/pii/B9780123970473000102

Chapter
5. CONCLUSIONS & FUTURE WORK

In this chapter…

The overall conclusions of the thesis have been summarized and proposed future work has been presented

5.1 Conclusions

Thermal sprayed coatings are widely used in the aerospace industry for tribological interfaces. Numerous studies have been conducted to discover the influence of different deposition parameters of APS and flame spraying on the wear performance of these coatings, especially at high temperatures. This thesis illustrates the successful HVOF deposition of nickel-graphite and copper-aluminum anti-wear coatings and their tribological behavior at room and elevated temperatures. The specific conclusions for each study have been summarized in their respective chapters. The overall conclusions of the thesis are summarized in this chapter:

1. Nickel graphite, HVOF sprayed coatings have shown promising results as wear resistant coatings due to their low wear volume loss at room temperature.

2. Ni-Graphite coatings deposited by means of HVOF were fully dense with small amount of oxygen and low coefficient of friction (i.e. as low as 0.2). A graphite-based tribofilm was responsible for reducing the coefficient of friction and protecting the surface from wear at room temperature. However, the friction and wear of these coatings increased when exposed to high temperatures (i.e. 450°C). The coefficient of friction and specific wear rate of both coatings were much higher at high temperatures compared to room temperature.

3. At room temperature, there was evidence of cracking and smeared debris, indicating that abrasive wear was the primary mechanism. At 450°C, wear was mainly caused by oxidative abrasion in both coatings, with an additional contribution from adhesion. The formation of an MML at higher temperatures did not protect the coating from wear and resulted in a higher

coefficient of friction and specific wear rate. This was attributed to the brittle nature of the nickel oxide formed at high temperatures.

4. Copper Aluminum coating deposited by HVOF were nearly fully dense, whereas the APS Cu-Al coating had a higher amount of porosity. XRD analysis indicated that the HVOF coating had less oxide formation than the APS coating. The HVOF coating had higher Vickers microhardness values than the APS coating at all tested temperatures due to its denser microstructure. The coefficients of friction for both coatings were much higher at room temperature than at higher temperatures. Additionally, the specific wear rates were the lowest at room temperature.

5. At room temperature, the HVOF and APS coatings displayed evidence of brittle fracture and interlamellar failure, respectively. This suggests that the primary wear mechanism was abrasive wear. At 300°C, the wear mechanism in the APS coating was dominated by abrasion, while in the HVOF coating, there was an additional contribution from adhesion. Abrasive wear seemed to be the primary wear mechanism at 450°C. The coating may have been protected from wear by the formation of a thin tribofilm layer at room temperature and 450°C. However, at 300°C, a thicker and more unstable mechanically mixed tribofilm layer may have caused more wear for both coatings.

6. Overall, the Ni-Graphite showed lower friction and wear compared to the Cu-Al (i.e. deposited by APS and HVOF) even though the hardness of the Ni-Graphite coatings is higher compared to that of the Cu-Al. This implies that the hardness is not the most suitable indicator for the wear behavior of these coatings. The difference in the tribological behavior between the two

coatings can rather be explained by the difference in interfacial processes and in-particular the graphite-based solid lubricant in the Ni-Graphite coatings.

5.2 Future Work

1. The optimal particle size distribution of the feedstock powder as well as the optimization of the HVOF spraying parameters would deserve further consideration, to explore possibly better coating wear properties.

2. Advanced tribological evaluation using application-relevant conditions should be performed in order to fully assess the capability of these coatings. In addition, tribological testing within-situ monitoring would be valuable to fully capture the interfacial processes.

3. Advanced ex-situ characterization investigation such as X-ray photoelectron spectroscopy and Raman spectroscopy should be conducted on the wear track of the coatings after testing to determine the components present in a substance (elemental composition) or on its surface and their chemical state.